

Mean Field Game Modeling of Overconfidence in Financial Markets

Lucas Sneller

Miami University, Oxford, OH 45056, USA

Abstract

This paper studies the effects of investor overconfidence on market dynamics through a mean field game (MFG) framework. Overconfidence is modeled as misperceived private-signal precision and analyzed in both static and dynamic settings. The static benchmark yields a closed-form linear price and transparent comparative statics in the overconfidence parameter. The dynamic model couples Bayesian filtering to endogenous stochastic price formation through an anchored-impact rule with mean-demand feedback. A checkable CARA best response under Gaussian price increments yields a linear feedback policy and a simple mean-field closure. Particle-based simulations distinguish *level amplification* (large mispricing/volatility levels driven by weak anchoring and high noise trading) from *overconfidence effects* (incremental differences when increasing k). Across a targeted joint grid over anchoring, impact, and noise trading, we find a robust negative result: overconfidence has economically small effects on price-level mispricing, while it strongly increases disagreement and trading intensity; mispricing levels are governed by the microstructure regime.

Keywords: Mean field games; McKean–Vlasov; overconfidence; behavioral finance; mispricing; volatility; heterogeneous beliefs; Bayesian filtering; Kalman–Bucy filter; endogenous price formation.

1 Introduction

Overconfidence—the tendency to overestimate one’s information precision or predictive ability—is a well-documented behavioral bias in financial markets and is empirically associated with excessive trading and episodes of mispricing Odean (1998); Barber and Odean (2001). Traditional financial models built around representative rational agents abstract from belief heterogeneity and endogenous feedback, limiting their ability to explain sustained deviations from fundamentals. This paper develops a mean field game (MFG) framework for a market populated by a continuum of overconfident agents, where each agent filters an unobserved fundamental from private signals and trades against an endogenous price impacted by mean demand.

Early behavioral models introduced stylized agent types (noise traders, momentum traders) to demonstrate how bounded rationality can drive prices away from fundamentals De Long et al. (1990); Hong and Stein (1999); Daniel et al. (1998); Gervais and Odean (2001), but typically rely on a small number of types rather than a full distribution of beliefs. Mean field games have been applied to financial markets in several contexts: Guéant, Lasry, and Lions Guéant et al. (2010) developed MFG frameworks for execution and portfolio problems; Carmona, Fouque, and Sun Carmona et al. (2015) studied systemic risk; Lachapelle et al. Lachapelle et al. (2016) applied MFG ideas to high-frequency trading and price formation; and Cardaliaguet and Lehalle Cardaliaguet and Lehalle (2018) analyzed trade crowding effects.

Our contribution relative to existing MFG finance literature is threefold: (i) we model overconfidence as misperceived private-signal precision and track its consequences through filtering,

belief dispersion, and demand; (ii) we use an explicitly stated stochastic price formation rule with endogenous impact from mean demand; (iii) we study a bounded-rational *myopic* mean-field consistent dynamics via particle simulations across bull/bear regimes. A central finding is a *robust negative result*: across a targeted joint grid over anchoring, impact, and noise trading, overconfidence has economically small effects on price-level mispricing, while it strongly increases disagreement and trading intensity; mispricing levels are governed by the microstructure regime. We distinguish *level amplification* (large mispricing/volatility levels driven by weak anchoring and high noise trading) from *overconfidence effects* (incremental differences when increasing k), showing that market microstructure parameters govern mispricing magnitudes while overconfidence primarily affects belief dispersion.

The paper's dynamic analysis has a deliberate two-model structure. (A) Our *computed* equilibrium concept is a discrete-time myopic mean-field consistent dynamics (Sections III and VI): this is the object behind all reported figures and tables. (B) As a theoretical benchmark, Section IV also derives an exact finite-horizon continuous-time CARA/LQG best response under partial information; this analytic extension clarifies how the full intertemporal solution adds a hedging correction to the myopic rule, but it is not what we simulate in Section VI.

The main contributions of this paper are:

- We formulate a mean field game with overconfident Bayesian filtering and an explicit stochastic price equation with endogenous impact from mean demand.
- We provide a clean static benchmark with a closed-form linear price (5) and explicit dependence on the overconfidence parameter k .
- In the dynamic setting, we derive a checkable myopic CARArule under Gaussian price increments and obtain a homogeneous mean-field closure (48) (with an associated stability condition).
- We report particle-based numerical experiments (large- N simulations) across bull/bear regimes and overconfidence levels, including mechanism diagnostics (belief dispersion and perceived uncertainty) and validation checks (convergence in N and sensitivity to impact strength).
- **Robust negative result:** Across a targeted joint grid over $(\kappa, \lambda, \sigma_\eta)$, overconfidence has economically small effects on price-level mispricing, while it strongly increases disagreement and trading intensity; mispricing levels are governed by the microstructure regime (Subsection 6.3.3).

The remainder of this paper is organized as follows. Section II presents the model, including the static benchmark and the dynamic price/belief dynamics. Section III discusses the mean-field object in the presence of common noise and the fixed-point notion of equilibrium. Section IV states the myopic equilibrium ingredients used for the numerical work and records the continuous-time CARA/LQG benchmark. Section V gives short proofs. Section VI presents numerical experiments, the empirical bridge (moment-match vignette), and the joint-grid analysis that delivers the robust negative result. Section VII concludes.

2 Problem Statement and Model

2.1 Setup and Notation

We consider a financial market with a continuum of investors indexed by $i \in [0, 1]$ over a horizon $[0, T]$. Let $(\Omega, \mathcal{F}, \{\mathcal{F}_t\}_{t \geq 0}, \mathbb{P})$ support independent Brownian motions W_t (fundamental shock),

Z_t (aggregate price/noise-trading shock), U_t (common signal component), and $\{B_{i,t}\}_{i \in [0,1]}$ (idiosyncratic signal noise). We write $\mathbb{E}[\cdot]$ for expectation and $\tau = 1/\sigma^2$ for precision.

Model parameters: $\gamma > 0$ (absolute risk aversion), $\kappa > 0$ (fundamental anchoring strength), $\lambda > 0$ (impact strength), $k \geq 1$ (overconfidence), and volatilities $\sigma_v, \sigma_c, \sigma_\epsilon, \sigma_\eta > 0$ (fundamental shock, common signal component, idiosyncratic signal noise, and price/noise-trading noise). Overconfidence is modeled as a misperception of private-signal precision: an agent with parameter k uses perceived idiosyncratic variance σ_ϵ^2/k in belief updating (equivalently, perceived precision k/σ_ϵ^2).

2.2 Static Benchmark

As a baseline, consider a static market with fundamental value $v \sim \mathcal{N}(\mu_v, \sigma_v^2)$. Each investor receives a private signal

$$s_i = v + \epsilon_i, \quad \epsilon_i \sim \mathcal{N}(0, \sigma_\epsilon^2), \quad (1)$$

and chooses demand x_i for a single risky asset with payoff v at settlement. Investors have CARUtility

$$U_i = -\mathbb{E}[e^{-\gamma W_i} | s_i], \quad W_i = w_0 + x_i(v - p), \quad (2)$$

and take the price impact rule (instantaneous clearing with noise demand)

$$p = \lambda \int_0^1 x_i di + \eta, \quad \eta \sim \mathcal{N}(0, \sigma_\eta^2). \quad (3)$$

Under Gaussian beliefs, maximizing CARUtility is equivalent to maximizing mean minus $(\gamma/2)$ times variance. With perceived signal precision $\tau'_\epsilon = k/\sigma_\epsilon^2$, the (perceived) posterior variance is $\sigma_{\text{post}}^2 = 1/(\tau_v + \tau'_\epsilon)$ and the posterior mean is $\hat{v}_i = (\tau_v \mu_v + \tau'_\epsilon s_i)/(\tau_v + \tau'_\epsilon)$. The optimal demand is therefore

$$x_i^* = \frac{\hat{v}_i - p}{\gamma \sigma_{\text{post}}^2}. \quad (4)$$

Taking $i \in [0, 1]$ and using $\int_0^1 s_i di = v$ almost surely, we obtain $\int_0^1 \hat{v}_i di = (\tau_v \mu_v + \tau'_\epsilon v)/(\tau_v + \tau'_\epsilon)$ and hence a closed-form linear price

$$\begin{aligned} p &= \frac{\lambda \tau'_\epsilon}{\gamma + \lambda(\tau_v + \tau'_\epsilon)} v + \frac{\gamma}{\gamma + \lambda(\tau_v + \tau'_\epsilon)} \eta \\ &\quad + \frac{\lambda \tau_v}{\gamma + \lambda(\tau_v + \tau'_\epsilon)} \mu_v. \end{aligned} \quad (5)$$

Equation (5) makes the channel explicit: higher k increases perceived precision τ'_ϵ and therefore strengthens the price response to v while also increasing demand magnitude for a given mispricing.

2.3 Dynamic Mean Field Game Formulation

2.3.1 State Dynamics and Mean-Field Coupling

The fundamental value follows a diffusion

$$dv_t = \mu_v dt + \sigma_v dW_t, \quad (6)$$

and each investor observes a private signal process

$$d\xi_{i,t} = v_t dt + \sigma_c dU_t + \sigma_\epsilon dB_{i,t}, \quad (7)$$

where $\{B_{i,t}\}$ are independent across i . The market price evolves endogenously through an anchored impact rule:

$$dp_t = \kappa(v_t - p_t) dt + \lambda\bar{x}_t dt + \sigma_\eta dZ_t, \quad \bar{x}_t := \int_0^1 x_{i,t} di. \quad (8)$$

Equation (8) is a reduced-form microstructure: prices mean-revert to fundamentals at rate κ (arbitrage/fundamental anchoring), respond to average demand with strength λ , and are perturbed by aggregate noise Z_t . The mean-field coupling enters through \bar{x}_t .

Microstructure sketch for the anchored impact rule. Equation (8) can be viewed as a reduced-form limit of competitive risk-neutral market making with inventory costs, plus an (exogenous) arbitrage/anchoring flow.

Linear impact from inventory-averse competitive market makers. Let Q_t denote aggregate net order flow hitting dealers (positive when the public buys), and let the representative dealer's inventory be q_t , with

$$dq_t = -dQ_t, \quad (\text{dealers take the opposite side of net flow}).$$

Assume dealers are risk-neutral and competitive (zero expected profit), but face a quadratic inventory holding cost $\frac{\phi}{2}q_t^2$. A standard myopic quoting / LQ argument implies the midprice is shifted linearly by inventory,

$$p_t \approx m_t - \phi q_t,$$

where m_t is the dealer's "efficient" benchmark (e.g., a fast-moving reference level). Differentiating and substituting $dq_t = -dQ_t$ gives

$$dp_t \approx dm_t + \phi dQ_t,$$

so that (in drift form) price changes are *linear* in contemporaneous net flow. Writing $dQ_t = \bar{x}_t dt + \sigma_Q dZ_t$ yields the impact and noise terms

$$dp_t \supset \lambda\bar{x}_t dt + \sigma_\eta dZ_t, \quad \lambda := \phi, \quad \sigma_\eta := \lambda\sigma_Q.$$

Anchoring as reduced-form arbitrage pressure. To capture fast arbitrage / fundamental anchoring, posit an additional "arbitrage" flow that leans against mispricing,

$$x_t^{\text{arb}} = a(v_t - p_t),$$

so total net flow is $\bar{x}_t + x_t^{\text{arb}}$ at the same impact slope λ . Then

$$dp_t \approx \lambda(\bar{x}_t + a(v_t - p_t)) dt + \sigma_\eta dZ_t = \kappa(v_t - p_t) dt + \lambda\bar{x}_t dt + \sigma_\eta dZ_t, \quad \kappa := \lambda a,$$

which matches the anchored impact specification.

2.3.2 Equilibrium Price Formation

We focus on feedback strategies where demand depends on perceived mispricing. Let $\hat{v}_{i,t}$ denote investor i 's Kalman-Bucy estimate of v_t under the *perceived* measurement-noise variance $R'(k)$ (Appendix A). When $k = 1$ this coincides with the true conditional mean $\mathbb{E}[v_t | \mathcal{F}_t^1]$; when $k \neq 1$ it should be interpreted as a *subjective* filter state computed under the investor's misperceived signal precision. Define the mean belief $m_t := \int_0^1 \hat{v}_{i,t} di$. A broad class of (best-response and learning-based) specifications take the form

$$x_{i,t} = \Theta_t(\Sigma_{i,t})(\hat{v}_{i,t} - p_t), \quad (9)$$

where $\Sigma_{i,t}$ is the agent's perceived posterior variance and $\Theta_t(\cdot)$ is increasing in perceived precision. In Section IV we derive an explicit myopic CARA best response that fits (9) and clarifies how overconfidence affects demand through belief updating (not through an additional ad hoc demand multiplier).

2.3.3 Belief Updating via Kalman Filtering

Each investor maintains a belief state $(\hat{v}_{i,t}, \Sigma_{i,t})$ where $\hat{v}_{i,t}$ is the posterior mean of v_t and $\Sigma_{i,t}$ is the perceived posterior variance. In the linear-Gaussian setting above, $(\hat{v}_{i,t}, \Sigma_{i,t})$ satisfy Kalman–Bucy equations driven by the private signal $\xi_{i,t}$. Overconfidence enters by replacing σ_ϵ^2 with σ_ϵ^2/k in the perceived filter. We summarize the resulting filter in Appendix A.

2.3.4 Objective Functional

Investor i chooses an adapted process $x_{i,t}$ (position). Rather than solving the full intertemporal exponential-utility control problem, we adopt a bounded-rational *myopic* approximation: at each time step, the investor selects $x_{i,t}$ to maximize conditional mean minus $(\gamma/2)$ times conditional variance of the next price increment. Section IV provides a checkable derivation and the resulting linear feedback rule.

2.3.5 Mean-Field Consistency (Myopic)

Let μ_t denote the (possibly random) law of $(\hat{v}_{i,t}, \Sigma_{i,t})$ across agents. Together with (8), we study a *myopic mean-field consistent* fixed point: (i) given a conjectured mean-field flow $\{\mu_t\}$ (equivalently, moments such as m_t), each agent applies the myopic CARA rule in Section IV; and (ii) the resulting population law induced by the controlled belief dynamics is consistent with $\{\mu_t\}$. Section III formalizes the mean-field object and discusses the common-noise aspect induced by W_t and Z_t .

3 Mean-Field Approximation and Limiting Equations

3.1 Mean-Field Object Under Common Noise

Because the model includes common shocks (W_t, U_t, Z_t) through the fundamental, correlated signals, and price noise, the appropriate mean-field object is the *conditional* population law given the common filtration $\mathcal{F}_t^0 := \sigma(W_s, U_s, Z_s : s \leq t)$. Concretely, let $X_{i,t} := (\hat{v}_{i,t}, \Sigma_{i,t}, k_i)$ denote investor i 's internal state (belief, perceived uncertainty, and overconfidence type), and define the mean-field flow

$$\mu_t := \mathcal{L}(X_{i,t} \mid \mathcal{F}_t^0). \quad (10)$$

The conditional mean belief $m_t := \int \hat{v} \mu_t(d\hat{v} d\Sigma dk)$ enters the price dynamics through $\bar{x}_t = \int x(t, \hat{v}, \Sigma, p_t, \mu_t) \mu_t(d\hat{v} d\Sigma dk)$.

3.2 Mean-Field Equilibrium (Common-Noise Formulation)

Fix a candidate flow $\{\mu_t\}_{t \in [0,T]}$ and the resulting price process $\{p_t\}$ from (8). In the bounded-rational formulation of this paper, the representative agent does not solve a full intertemporal control problem; instead, given $\{\mu_t\}$ and $\{p_t\}$ the agent applies the myopic rule from Section IV, yielding a feedback $x_{i,t} = x^{\text{myopic}}(t, X_{i,t}, p_t, \mu_t)$. The induced controlled state process generates a new conditional flow $\{\tilde{\mu}_t\}$. A myopic mean-field equilibrium is a fixed point $\mu = \tilde{\mu}$.

In common-noise settings, μ_t is random and its evolution is governed by a stochastic Kolmogorov forward equation (stochastic Fokker–Planck / SPDE) for the conditional law; see, e.g.,

Carmona and Delarue (2018a); Lacker (2016). In Section VI we compute equilibrium statistics using a particle approximation: simulate a large N -agent system driven by shared (W, Z) and independent $\{B_i\}$ and estimate μ_t via the empirical measure.

Scope of theoretical results. To avoid confusion, we explicitly state what this paper proves and what it does not claim. **What we prove:** Under the condition $\gamma\sigma_\eta^2 > \lambda$, Theorem 3.2 establishes (i) well-posedness of the N -agent system and the mean-field limit, (ii) existence and uniqueness of the myopic mean-field fixed point \bar{x}_t given by (20), and (iii) convergence of the N -particle empirical measure to the conditional law μ_t (conditional propagation of chaos). **What we do not claim:** This paper does not establish existence or uniqueness of a full optimal-control MFG equilibrium under intertemporal exponential utility maximization with endogenous filtering on prices. The myopic rule (29) is a bounded-rational approximation that yields a tractable closed-form mean-field closure; Subsection 4.3 discusses an intertemporal CARA/LQG extension as a constructive comparison, but a complete verification of existence/uniqueness conditions for that intertemporal MFG coupling would strengthen the theoretical foundation (see Section VII).

3.3 Discrete-Time Myopic Mean-Field Equilibrium (What We Compute)

The numerical experiments in Section VI implement a discrete-time, bounded-rational equilibrium concept consistent with the myopic rule in Section IV. Fix a time grid $t = 0, 1, \dots, T$ (step size $\Delta t = 1$ in the implementation) and consider the N -agent system induced by: (i) fundamental and price updates (Euler discretization of (8)), (ii) private-signal observations and Kalman belief updates (Appendix A), and (iii) the myopic trading rule (29).

Definition (myopic mean-field equilibrium, discrete time). Given a conjectured mean-field action \bar{x}_t and public price p_t , agent i computes a belief state $(\hat{v}_{i,t}, \Sigma_{i,t})$ and chooses $x_{i,t}$ according to the myopic mean-variance rule. A discrete-time myopic mean-field equilibrium at time t is a fixed point $\bar{x}_t = \frac{1}{N} \sum_{i=1}^N x_{i,t}$ under this rule. In the implementation, the rule is linear in \bar{x}_t and the fixed point is computed in closed form (Proposition 4.5).

3.4 Discrete-Time Well-Posedness (Existence and Uniqueness of Paths)

We formalize the particle implementation as a coupled discrete-time dynamical system on a fixed time grid.

Assumptions. Fix $T \in \mathbb{N}$ and $\Delta t > 0$ and assume: (A1) parameters satisfy $\kappa > 0$, $\sigma_\eta > 0$, $\gamma > 0$, $\alpha_0 > 0$ and initial conditions $(v_0, p_0, \{\hat{v}_{i,0}, \Sigma_{i,0}\}_{i=1}^N)$ are finite with $\Sigma_{i,0} \geq 0$; (A2) beliefs evolve via the discrete-time Kalman recursion in Appendix A (so $(\hat{v}_{i,t}, \Sigma_{i,t})$ is uniquely defined given $(\hat{v}_{i,t-1}, \Sigma_{i,t-1})$ and the signal); (A3) for each t , the per-step mean-field map admits a unique fixed point \bar{x}_t (e.g., the contraction condition in Theorem 4.6 holds); (A4) price and fundamental updates are given by the Euler discretizations of their SDEs driven by specified shock sequences.

Theorem 3.1 (Well-posedness of the discrete-time particle system). *Under (A1)–(A4), for any realization of the common and idiosyncratic shock sequences, the discrete-time system defined by: (i) belief update (Appendix A), (ii) per-step myopic mean-field fixed point (Proposition 4.5), and (iii) Euler updates for (v_t, p_t) , admits a unique adapted solution path*

$$(v_t, p_t, \{\hat{v}_{i,t}, \Sigma_{i,t}\}_{i=1}^N, \bar{x}_t)_{t=0}^T.$$

3.5 Common-noise mean-field limit: fixed-point verification

This subsection records a self-contained fixed-point verification for the common-noise mean-field limit under the (myopic) CARA best response used throughout Sections III–IV. The key point

is that, in our information simplification (filtering on ξ^i only), the belief state dynamics are *conditionally i.i.d.* given the common filtration, so the mean-field object is the conditional law and the equilibrium closure reduces to an explicit algebraic fixed point.

Common and idiosyncratic noises. Recall the common filtration

$$\mathcal{F}_t^0 := \sigma(W_s, U_s, Z_s : s \leq t),$$

and idiosyncratic signal noises $\{B^i\}_{i \geq 1}$ independent across i and independent of (W, U, Z) .

Finite- N (continuous-time) price-taking system. Consider the N -agent system (continuous time) with a *price-taking* interaction through the average demand $\bar{x}_t^N := \frac{1}{N} \sum_{j=1}^N x_t^{j,N}$:

$$dv_t = \mu_v dt + \sigma_v dW_t, \quad (11)$$

$$d\xi_t^i = v_t dt + \sigma_c dU_t + \sigma_\epsilon dB_t^i, \quad i = 1, \dots, N, \quad (12)$$

$$dp_t^N = \kappa(v_t - p_t^N) dt + \lambda \bar{x}_t^N dt + \sigma_\eta dZ_t. \quad (13)$$

Agents compute the subjective Kalman–Bucy filter (Appendix A) from (12):

$$\begin{aligned} d\hat{v}_t^i &= \mu_v dt + K_t^{(i)}(d\xi_t^i - \hat{v}_t^i dt), \\ K_t^{(i)} &:= \frac{\Sigma_t^{(i)}}{R'_i}, \quad R'_i := \sigma_c^2 + \sigma_\epsilon^2/k_i. \end{aligned} \quad (14)$$

with Riccati $\dot{\Sigma}_t^{(i)} = \sigma_v^2 - (\Sigma_t^{(i)})^2/R'_i$ and $\Sigma_0^{(i)} \geq 0$. (For a homogeneous population, $k_i \equiv k$ and hence $K_t^{(i)} \equiv K_t$ and $\Sigma_t^{(i)} \equiv \Sigma_t$ are deterministic.)

Given (p_t^N, \bar{x}_t^N) , the myopic CARA rule (Proposition 4.2) prescribes the pointwise best response

$$x_t^{i,N} = \frac{\kappa(\hat{v}_t^i - p_t^N) + \lambda \bar{x}_t^N}{\gamma \sigma_\eta^2}, \quad i = 1, \dots, N. \quad (15)$$

Averaging (15) yields the *per-time* fixed point

$$(\gamma \sigma_\eta^2 - \lambda) \bar{x}_t^N = \kappa(\hat{m}_t^N - p_t^N), \quad \hat{m}_t^N := \frac{1}{N} \sum_{i=1}^N \hat{v}_t^i, \quad (16)$$

so whenever $\gamma \sigma_\eta^2 > \lambda$,

$$\bar{x}_t^N = \frac{\kappa}{\gamma \sigma_\eta^2 - \lambda} (\hat{m}_t^N - p_t^N). \quad (17)$$

Mean-field (conditional-law) system. Define the representative-agent belief state \hat{v}_t solving (14) with an independent copy B (and the same common noises (W, U, Z)), and define the conditional flow

$$\begin{aligned} \mu_t &:= \mathcal{L}(\hat{v}_t, \Sigma_t, k \mid \mathcal{F}_t^0), \\ m_t &:= \int \hat{v} \mu_t(d\hat{v} d\Sigma dk) = \mathbb{E}[\hat{v}_t \mid \mathcal{F}_t^0]. \end{aligned}$$

The mean-field price satisfies

$$dp_t = \kappa(v_t - p_t) dt + \lambda \bar{x}_t dt + \sigma_\eta dZ_t, \quad (18)$$

where \bar{x}_t is required to satisfy the mean-field consistency condition

$$\bar{x}_t = \int \frac{\kappa(\hat{v} - p_t) + \lambda\bar{x}_t}{\gamma\sigma_\eta^2} \mu_t(d\hat{v} d\Sigma dk). \quad (19)$$

Since only the mean of \hat{v} enters (19), the fixed point reduces to

$$\bar{x}_t = \frac{\kappa}{\gamma\sigma_\eta^2 - \lambda} (m_t - p_t), \quad \text{assuming } \gamma\sigma_\eta^2 > \lambda. \quad (20)$$

Theorem 3.2 (Common-noise fixed point and mean-field limit). *Assume $\gamma\sigma_\eta^2 > \lambda$ and $\sup_{i \leq N} \mathbb{E}[|\hat{v}_0^i|^2] < \infty$ with $\sup_{i \leq N} \Sigma_0^{(i)} < \infty$ (and, for simplicity, i.i.d. initial belief states across i conditional on \mathcal{F}_0^0). Then:*

- (i) (Well-posedness.) *The N -agent system (11)–(13) with controls given by the myopic fixed point (15) admits a unique strong solution, and the limiting system (11)–(18) with \bar{x} given by (20) admits a unique strong solution.*
- (ii) (Fixed-point verification.) *The process \bar{x} defined by (20) is the unique solution to the mean-field consistency equation (19) (i.e., a unique myopic common-noise MFG fixed point).*
- (iii) (Conditional propagation of chaos / LLN.) *Let the empirical measure of belief states be $\mu_t^N := \frac{1}{N} \sum_{i=1}^N \delta_{(\hat{v}_t^i, \Sigma_t^{(i)}, k_i)}$. Then for each fixed t ,*

$$\mu_t^N \xrightarrow[N \rightarrow \infty]{} \mu_t \quad \text{in probability, and} \quad \hat{m}_t^N \rightarrow m_t \text{ in } L^2.$$

Consequently, $\bar{x}_t^N \rightarrow \bar{x}_t$ in L^2 and $p_t^N \rightarrow p_t$ in L^2 uniformly on $[0, T]$.

Proof. Step 1 (Well-posedness). For each i , the filter SDE (14) is linear with adapted coefficients and admits a unique strong solution with finite second moments; the Riccati equation is a scalar ODE with global solution (Appendix A). Given \bar{x}^N and p^N , the control (15) is affine in $(\hat{v}^i, p^N, \bar{x}^N)$. The averaging identity (16) yields the explicit closure (17) when $\gamma\sigma_\eta^2 > \lambda$. Substituting (17) into (13) gives a linear SDE for p^N driven by (W, U, Z) and the averaged belief \hat{m}^N , hence a unique strong solution. The limiting system is identical with $(\hat{m}^N, \bar{x}^N, p^N)$ replaced by (m, \bar{x}, p) .

Step 2 (Fixed point). Equation (19) is affine in \bar{x}_t :

$$\bar{x}_t = \frac{\kappa(m_t - p_t) + \lambda\bar{x}_t}{\gamma\sigma_\eta^2}.$$

Rearranging gives $(\gamma\sigma_\eta^2 - \lambda)\bar{x}_t = \kappa(m_t - p_t)$ and thus (20). Uniqueness follows since $\gamma\sigma_\eta^2 - \lambda > 0$.

Step 3 (Conditional LLN / propagation of chaos). Conditional on \mathcal{F}_t^0 , the idiosyncratic noises $\{B^i\}$ are independent and the filter equations (14) are driven by independent Brownian motions with the same common coefficients and common path (W, U, Z) . Hence the collection $\{(\hat{v}_t^i, \Sigma_t^{(i)}, k_i)\}_{i=1}^N$ is i.i.d. conditional on \mathcal{F}_t^0 (with law μ_t), and the conditional law of large numbers implies $\mu_t^N \Rightarrow \mu_t$ and

$$\mathbb{E}[|\hat{m}_t^N - m_t|^2 | \mathcal{F}_t^0] = \frac{1}{N} \text{Var}(\hat{v}_t | \mathcal{F}_t^0),$$

so $\hat{m}_t^N \rightarrow m_t$ in L^2 . Using (17)–(20) then gives $\bar{x}_t^N \rightarrow \bar{x}_t$ in L^2 .

Step 4 (Price convergence). Subtract (18) from (13) to get $d(p_t^N - p_t) = -\kappa(p_t^N - p_t) dt + \lambda(\bar{x}_t^N - \bar{x}_t) dt$. By Grönwall and Cauchy–Schwarz,

$$\sup_{t \leq T} \mathbb{E}|p_t^N - p_t|^2 \leq C_T \int_0^T \mathbb{E}|\bar{x}_s^N - \bar{x}_s|^2 ds \xrightarrow[N \rightarrow \infty]{} 0,$$

and the L^2 uniform convergence follows. \square

Remark 3.3 (Stochastic Fokker–Planck equation for μ_t). For any test function $\varphi \in C_b^2(\mathbb{R} \times \mathbb{R}_+ \times \mathbb{R}_+)$, the conditional law $\mu_t = \mathcal{L}(\hat{v}_t, \Sigma_t, k \mid \mathcal{F}_t^0)$ satisfies the common-noise SPDE (in weak form)

$$\begin{aligned} d\langle \mu_t, \varphi \rangle &= \left\langle \mu_t, (\mu_v + K_t(k)(v_t - \hat{v})) \partial_{\hat{v}} \varphi \right. \\ &\quad \left. + \frac{1}{2} K_t(k)^2 \sigma_c^2 \partial_{\hat{v}\hat{v}}^2 \varphi \right\rangle dt \\ &\quad + \left\langle \mu_t, K_t(k) \sigma_c \partial_{\hat{v}} \varphi \right\rangle dU_t. \end{aligned}$$

where $\langle \mu, \varphi \rangle := \int \varphi d\mu$ and $K_t(k) = \Sigma_t(k) / (\sigma_c^2 + \sigma_\epsilon^2/k)$. In the homogeneous case, μ_t is Gaussian in \hat{v} conditional on \mathcal{F}_t^0 (with random mean m_t).

3.6 Mean-Field Limit

We state a standard common-noise McKean–Vlasov/MFG limit as a black-box framework; our contribution is the constructive solution in the LQG specialization, given in Section 3.7.

Setting. Consider a common-noise McKean–Vlasov system on a finite horizon $[0, T]$. Let $\mathcal{F}_t^0 := \sigma(W_s^0 : s \leq t)$ be the filtration generated by a common Brownian motion W^0 , and for each $N \geq 1$ let $\{B^i\}_{i=1}^N$ be mutually independent and independent of W^0 . The N -agent state processes $\{X_t^{i,N}\}_{i=1}^N$ take values in \mathbb{R}^d and satisfy a coupled system whose coefficients may depend on the empirical measure $\bar{\mu}_t^N := \frac{1}{N} \sum_{j=1}^N \delta_{X_t^{j,N}}$ and on the common noise. The mean-field limit is described by a McKean–Vlasov SDE in which the conditional law $\mu_t = \mathcal{L}(X_t \mid \mathcal{F}_t^0)$ of a representative state X_t enters the drift and diffusion; see Carmona and Delarue (2018a,b); Lacker (2018).

Assumptions. We impose the following standard conditions (see, e.g., Fournier and Guillin (2015); Lacker (2018)).

- (H1) (**Lipschitz in state and measure.**) The drift $b(t, x, \mu)$ and diffusion $\sigma(t, x, \mu)$ are Lipschitz in (x, μ) uniformly in $t \in [0, T]$, with μ in the space of probability measures on \mathbb{R}^d metrized by the Wasserstein distance W_2 .
- (H2) (**Linear growth.**) $|b(t, x, \mu)| + \|\sigma(t, x, \mu)\| \leq C(1 + |x| + W_2(\mu, \delta_0))$ for some $C \geq 0$.
- (H3) (**Common noise integrability.**) Common-noise coefficients are progressively measurable and square-integrable on $[0, T]$ a.s.
- (H4) (**Initial condition.**) The initial states $\{X_0^{i,N}\}_{i=1}^N$ are i.i.d. with law μ_0 and satisfy $\mathbb{E}[|X_0^{i,N}|^2] < \infty$; μ_0 has finite second moment.
- (H5) (**Non-degeneracy / bounded coefficients.**) The diffusion matrix $\sigma\sigma^\top$ is uniformly elliptic (or at least non-degenerate) and all coefficients are bounded when restricted to compacts in $\mathbb{R}^d \times \mathcal{P}_2(\mathbb{R}^d)$.

Under (H1)–(H5), the limiting McKean–Vlasov equation admits a unique strong solution and the N -particle system is well-posed; see Carmona and Delarue (2018a,b).

Theorem 3.4 (Convergence of empirical measures). *Assume (H1)–(H5). Let $\{X^{i,N}\}_{i=1}^N$ solve the N -particle system and let X solve the limiting McKean–Vlasov equation with the same common noise W^0 and i.i.d. copies $\{B^i\}$ of the idiosyncratic driver. Then for each $t \in [0, T]$,*

$$\bar{\mu}_t^N \xrightarrow[N \rightarrow \infty]{W_2} \mu_t \quad \text{in probability},$$

where $\mu_t = \mathcal{L}(X_t | \mathcal{F}_t^0)$ is the conditional law of the limit process. In particular, propagation of chaos holds: any fixed finite marginals converge in law to the product of the limit conditional law.

Proof sketch (black-box references). Existence and uniqueness for the limit equation follow from (H1)–(H2) and fixed-point arguments in the space of flows of measures; see Carmona and Delarue (2018a). Convergence of $\bar{\mu}_t^N$ to μ_t in W_2 is a standard consequence of (H1)–(H5) and the conditional law of large numbers for the empirical measure; see Fournier and Guillin (2015) for quantitative rates and Lacker (2018) for the common-noise formulation. Propagation of chaos is then implied by the same estimates; see Carmona and Delarue (2018b). \square

Proposition 3.5 (Stability of mean-field equilibrium). *Under (H1)–(H5), the mean-field equilibrium flow $\{\mu_t\}_{t \in [0, T]}$ is unique in the class of admissible flows with finite second moments. Moreover, $\sup_{t \in [0, T]} \mathbb{E}[W_2(\bar{\mu}_t^N, \mu_t)^2] \leq C/N$ for some constant C depending on T and the data.*

Proof sketch (black-box references). Uniqueness follows from the Lipschitz structure (H1) and Gronwall-type estimates in Wasserstein space; see Carmona and Delarue (2018a). The $O(1/N)$ bound for $\mathbb{E}[W_2(\bar{\mu}_t^N, \mu_t)^2]$ is given in Fournier and Guillin (2015) and Huang et al. (2006) for the classical and MFG settings. \square

Remark 3.6 (LQG specialization). In our LQG setting (see Section IV), the coefficients are affine in state and measure, so (H1)–(H2) hold and the limit is explicit. The preceding black-box statements justify using the mean-field system as the large- N approximation for the particle implementation in Section VI.

3.7 Constructive LQG Solution via Picard Iteration

Endogenous vs exogenous. Mean demand \bar{x} , price p , and (from the equilibrium map) mispricing $\bar{y} = m - p$ and the coefficient B_t (driven by \bar{x}) are *endogenous*; in equilibrium, beliefs and the filter are consistent with the chosen information. Exogenous parameters include $\kappa, \lambda, \sigma_\eta, \gamma$, and other primitives (e.g. $\sigma_v, \sigma_c, \sigma_\epsilon, k$). In this formulation, belief updating conditions only on the private signal ξ and not on the price observation channel; hence the mean belief m_t is not fed back by \bar{x} . Price is endogenous as an outcome of \bar{x} but is not used as an observation in the filter; incorporating it would require joint filtering and a richer fixed-point formulation (see Section IV).

Reduced state and dynamics. Define the (belief–price) mispricing state

$$y_t := \hat{v}_t - p_t. \quad (21)$$

We work in the homogeneous representative-agent setting with overconfidence parameter k , so \hat{v}_t is the subjective Kalman estimate of v_t , Σ_t is the perceived posterior variance, and $R' := \sigma_c^2 + \sigma_\epsilon^2/k$ is the perceived measurement-noise variance. Wealth and state dynamics in innovation form are

$$dW_t = x_t (\kappa y_t + \lambda \bar{x}_t) dt + x_t \sigma_\eta dI_t^p, \quad (22)$$

$$dy_t = (\mu_v - \kappa y_t - \lambda \bar{x}_t) dt + \beta_t dI_t^\xi - \sigma_\eta dI_t^p, \quad (23)$$

where I^p and I^ξ are independent Brownian motions (price and signal innovations). The (subjective) unhedgeable loading is

$$\beta_t = K_t \sqrt{\sigma_c^2 + \sigma_\epsilon^2}, \quad K_t = \frac{\Sigma_t}{R'}, \quad R' = \sigma_c^2 + \frac{\sigma_\epsilon^2}{k}, \quad (24)$$

and the perceived posterior variance Σ_t solves the Riccati equation

$$\dot{\Sigma}_t = \sigma_v^2 - \frac{\Sigma_t^2}{R'}, \quad \Sigma_0 \geq 0. \quad (25)$$

Fixed-point map and contraction. Theorem 3.4 provides the framework: existence, uniqueness, and convergence of the mean-field limit are from the black-box theory (assumptions (H1)–(H5)); the reduced dynamics (22)–(23), Riccati (25), and mean-field update (26) below are derived in our LQG setting. Given a candidate mean-field demand process $\bar{x}(\cdot)$, one can (i) solve the backward Riccati for A_t (independent of \bar{x}), (ii) solve the backward linear ODE for B_t driven by \bar{x}_t , (iii) simulate forward the coupled (v_t, m_t, p_t) and hence $\bar{y}_t = m_t - p_t$, and (iv) update \bar{x} via the mean-field consistency relation. This defines a fixed-point map Φ on trajectories $\bar{x}(\cdot)$.

Fixed-point object. The fixed-point object is the map Φ on the space $\mathcal{X} := L_{\mathcal{F}^0}^\infty(\Omega \times [0, T])$ of candidate mean-field demand trajectories (adapted to the common filtration \mathcal{F}^0), equipped with the norm $\|\bar{x}\|_\infty := \text{ess sup}_{(\omega, t) \in \Omega \times [0, T]} |\bar{x}_t(\omega)|$. Equilibrium corresponds to the unique fixed point $\bar{x}^* = \Phi(\bar{x}^*)$ when the contraction condition $q < 1$ below holds; see Proposition 3.7.

Proposition 3.7 (Constructive equilibrium under weak coupling / small horizon). *Define the fixed-point map Φ on $\bar{x}(\cdot)$ as follows. Given $\bar{x}(\cdot)$:*

- (i) *Solve backward the Riccati equation for A_t with terminal condition $A_T = 0$ (as in the A-ODE of the exact CARA/LQG formulation).*
- (ii) *Solve backward the linear ODE for B_t driven by \bar{x}_t , with terminal condition $B_T = 0$.*
- (iii) *Solve forward the dynamics for (v_t, m_t, p_t) given \bar{x}_t , and set $\bar{y}_t = m_t - p_t$.*
- (iv) *Update via mean-field consistency:*

$$\bar{x}_t = \frac{(\kappa + \sigma_\eta^2 A_t) \bar{y}_t + \sigma_\eta^2 B_t}{\gamma \sigma_\eta^2 - \lambda}. \quad (26)$$

Define

$$q := \frac{\lambda T}{\gamma \sigma_\eta^2 - \lambda} (2\kappa + \kappa^2 T). \quad (27)$$

If $\gamma \sigma_\eta^2 > \lambda$ and $q < 1$, then Φ is a contraction on the space $\mathcal{X} := L_{\mathcal{F}^0}^\infty(\Omega \times [0, T])$ and the fixed point exists and is unique; Picard iteration converges.

Proof. We make the contraction argument fully explicit.

Functional-analytic setup. Fix a filtered probability space $(\Omega, \mathcal{F}, \mathcal{F}^0, \mathbb{P})$ supporting the common shocks (e.g. (W, U, Z) as in (30)–(32)) and the cross-sectional private noises. Let $\mathcal{F}^0 = (\mathcal{F}_t^0)_{t \in [0, T]}$ be the (common) market filtration containing the common shocks. Define the Banach space

$$\mathcal{X} := L_{\mathcal{F}^0}^\infty(\Omega \times [0, T]), \quad \|\bar{x}\|_\infty := \text{ess sup}_{(\omega, t) \in \Omega \times [0, T]} |\bar{x}_t(\omega)|.$$

(If one prefers to restrict to deterministic mean-field trajectories $\bar{x} : [0, T] \rightarrow \mathbb{R}$, the same proof applies verbatim with the usual sup norm.)

Assume $\gamma \sigma_\eta^2 > \lambda$, so the denominator in (26) is strictly positive. Also assume β is \mathcal{F}^0 -progressively measurable and bounded on $[0, T]$ (this holds under the constant-gain closure (48), or any bounded-gain filtering specification used in Sections III–IV).

Step 1: Riccati well-posedness and a uniform bound for A . In the homogeneous case, A_t solves (42) with terminal condition $A_T = 0$:

$$-\dot{A}_t = \frac{\kappa^2}{\sigma_\eta^2} - \beta_t^2 A_t^2, \quad A_T = 0.$$

Set $\tilde{A}_s := A_{T-s}$ for $s \in [0, T]$. Then

$$\dot{\tilde{A}}_s = \frac{\kappa^2}{\sigma_\eta^2} - \beta_{T-s}^2 \tilde{A}_s^2, \quad \tilde{A}_0 = 0.$$

Nonnegativity. If $\tilde{A}_s < 0$ at some s , then $\dot{\tilde{A}}_s = \frac{\kappa^2}{\sigma_\eta^2} - \beta_{T-s}^2 \tilde{A}_s^2 \geq \frac{\kappa^2}{\sigma_\eta^2} > 0$, so the trajectory is strictly increasing whenever it is negative. Since $\tilde{A}_0 = 0$, it follows that $\tilde{A}_s \geq 0$ for all $s \in [0, T]$, hence $A_t \geq 0$ for all t . *Coarse bound.* Because the quadratic term is nonnegative,

$$\dot{\tilde{A}}_s \leq \frac{\kappa^2}{\sigma_\eta^2} \implies 0 \leq \tilde{A}_s \leq \frac{\kappa^2}{\sigma_\eta^2} s,$$

hence

$$0 \leq A_t \leq \frac{\kappa^2}{\sigma_\eta^2} (T-t) \leq \frac{\kappa^2}{\sigma_\eta^2} T \quad \text{for all } t \in [0, T].$$

In particular, $A \in L^\infty([0, T])$ and $\|A\|_\infty \leq \kappa^2 T / \sigma_\eta^2$.

Step 2: Precise assumption on mean belief and the \bar{y} -Lipschitz bound. Recall $\bar{y}_t := m_t - p_t$ in Proposition III.7.

In the myopic formulation of Section IV.B, belief updating (Appendix A) is conditioned only on the private signal $\xi_{i,t}$ (and not on the endogenous price observation channel). Under this modeling choice, the mean belief process $m_t = \int_0^1 \hat{v}_{i,t} di$ is independent of the mean-field demand input \bar{x} ; i.e. for two inputs $\bar{x}, \bar{x}' \in \mathcal{X}$ we have $m \equiv m'$.

(If one prefers not to hard-code this, it suffices to assume instead that $\bar{x} \mapsto m$ is Lipschitz in $\|\cdot\|_\infty$ with constant $C_m T$; the bound below then holds with λ replaced by $\lambda + C_m$.)

Now fix $\bar{x}, \bar{x}' \in \mathcal{X}$. Couple the two forward systems on the same probability space with the same common shocks and identical initial conditions (v_0, p_0) . Subtracting the price equations (32) yields, pathwise,

$$d(p_t - p'_t) = -\kappa(p_t - p'_t) dt + \lambda(\bar{x}_t - \bar{x}'_t) dt, \quad (p_0 - p'_0) = 0,$$

since the common noise term $\sigma_\eta dZ_t$ cancels under this coupling. Solving gives

$$|p_t - p'_t| \leq \lambda \int_0^t e^{-\kappa(t-s)} |\bar{x}_s - \bar{x}'_s| ds \leq \lambda \int_0^t |\bar{x}_s - \bar{x}'_s| ds \leq \lambda T \|\bar{x} - \bar{x}'\|_\infty.$$

Because $m \equiv m'$, we have $\bar{y} - \bar{y}' = -(p - p')$, hence

$$\|\bar{y} - \bar{y}'\|_\infty \leq \lambda T \|\bar{x} - \bar{x}'\|_\infty.$$

Step 3: B -Lipschitz bound in \bar{x} . Given A (which does not depend on \bar{x}) and β (independent of \bar{x} under the same information closure as above), B_t solves (43) with terminal condition $B_T = 0$:

$$-\dot{B}_t = \frac{\kappa\lambda}{\sigma_\eta^2} \bar{x}_t + \mu_v A_t - \beta_t^2 A_t B_t, \quad B_T = 0.$$

(If β is allowed to depend on \bar{x} , an additional Lipschitz term appears; the same contraction logic goes through with a larger constant.)

Let B, B' be the solutions corresponding to \bar{x}, \bar{x}' and set $\Delta B := B - B'$. Subtracting the ODEs gives

$$-\dot{\Delta B}_t = \frac{\kappa\lambda}{\sigma_\eta^2} (\bar{x}_t - \bar{x}'_t) - \beta_t^2 A_t \Delta B_t, \quad \Delta B_T = 0.$$

By integrating factor,

$$\Delta B_t = \frac{\kappa\lambda}{\sigma_\eta^2} \int_t^T \exp\left(-\int_t^s \beta_u^2 A_u du\right) (\bar{x}_s - \bar{x}'_s) ds.$$

Since $A_u \geq 0$ and $\beta_u^2 \geq 0$, the exponential factor is at most 1, yielding

$$\|B - B'\|_\infty \leq \frac{\kappa\lambda}{\sigma_\eta^2} T \|\bar{x} - \bar{x}'\|_\infty.$$

Step 4: Contraction estimate for Φ and a fully checkable sufficient condition. Recall (26):

$$\Phi(\bar{x})_t = \frac{(\kappa + \sigma_\eta^2 A_t)\bar{y}_t + \sigma_\eta^2 B_t}{\gamma\sigma_\eta^2 - \lambda}.$$

Using $\gamma\sigma_\eta^2 - \lambda > 0$, boundedness of A , and the triangle inequality,

$$\|\Phi(\bar{x}) - \Phi(\bar{x}')\|_\infty \leq \frac{(\kappa + \sigma_\eta^2 \|A\|_\infty)\|\bar{y} - \bar{y}'\|_\infty + \sigma_\eta^2 \|B - B'\|_\infty}{\gamma\sigma_\eta^2 - \lambda}.$$

Substituting the bounds from Steps 2–3 gives

$$\|\Phi(\bar{x}) - \Phi(\bar{x}')\|_\infty \leq \frac{\lambda T}{\gamma\sigma_\eta^2 - \lambda} \left(2\kappa + \sigma_\eta^2 \|A\|_\infty\right) \|\bar{x} - \bar{x}'\|_\infty.$$

Finally, using $\|A\|_\infty \leq \kappa^2 T / \sigma_\eta^2$ from Step 1 yields the parameter-only bound

$$\|\Phi(\bar{x}) - \Phi(\bar{x}')\|_\infty \leq q \|\bar{x} - \bar{x}'\|_\infty, \quad q := \frac{\lambda T}{\gamma\sigma_\eta^2 - \lambda} \left(2\kappa + \kappa^2 T\right),$$

which is fully checkable from primitives.

Step 5: Banach fixed point. If $q < 1$, then Φ is a contraction on $(\mathcal{X}, \|\cdot\|_\infty)$, hence admits a unique fixed point $\bar{x}^* \in \mathcal{X}$. Moreover, the Picard iteration $\bar{x}^{n+1} = \Phi(\bar{x}^n)$ converges geometrically to \bar{x}^* in $\|\cdot\|_\infty$.

Remark (relation to the simpler myopic scaling). In the myopic closure where hedging terms are suppressed ($A \equiv 0, B \equiv 0$), the Lipschitz estimate tightens to a pure $O(T)$ scaling proportional to $\kappa\lambda / (\gamma\sigma_\eta^2 - \lambda)$, matching the heuristic small-horizon/weak-coupling condition discussed around (27). \square

Picard iteration. A conservative Lipschitz bound is q in (27); for $q < 1$, Banach yields uniqueness. Algorithm 1 summarizes the procedure. We initialize a candidate $\bar{x}^0(\cdot)$ (e.g., identically zero or the myopic closure $\bar{x}_t^0 = \kappa\bar{y}_t^0 / (\gamma\sigma_\eta^2 - \lambda)$) from a forward run with $\bar{x} \equiv 0$, then iterate: compute Σ, K, β from (25)–(24), solve A backward, solve B backward using the current \bar{x}^n , forward-simulate (v, m, p) and \bar{y}^n , update \bar{x}^{n+1} via (26), and stop when the residual (e.g., $\|\bar{x}^{n+1} - \bar{x}^n\|$ in L^2 or sup-norm over the time grid) is below a tolerance.

Implementation and reproducibility. The Picard iteration in Algorithm 1 is implemented in a MATLAB script; the path and run instructions will be specified in the replication package. All reported equilibrium paths and statistics use this routine with a fixed tolerance and time discretization.

Algorithm 1 Picard iteration for LQG mean-field equilibrium

- 1: **Input:** Horizon T , parameters $(\kappa, \lambda, \gamma, \sigma_\eta, \mu_v, \sigma_v, \sigma_c, \sigma_\epsilon, k)$, initial conditions $(v_0, p_0, \hat{v}_0, \Sigma_0)$, tolerance ϵ , max iterations N_{\max} .
 - 2: **Initialize:** Set $\bar{x}_t^0 \leftarrow 0$ (or myopic seed) for $t \in [0, T]$. Set $n \leftarrow 0$.
 - 3: **repeat**
 - 4: Compute Σ_t, K_t, β_t on $[0, T]$ from (25) and (24).
 - 5: Solve backward for A_t (Riccati, $A_T = 0$).
 - 6: Solve backward for B_t given \bar{x}_t^n (linear ODE, $B_T = 0$).
 - 7: Forward-simulate (v_t, m_t, p_t) and $\bar{y}_t^n = m_t - p_t$ using \bar{x}_t^n in the dynamics.
 - 8: Update $\bar{x}_t^{n+1} \leftarrow \frac{(\kappa + \sigma_\eta^2 A_t) \bar{y}_t^n + \sigma_\eta^2 B_t}{\gamma \sigma_\eta^2 - \lambda}$ for $t \in [0, T]$.
 - 9: Compute residual $r_n \leftarrow \|\bar{x}^{n+1} - \bar{x}^n\|$ (e.g., L^2 or sup over grid).
 - 10: $n \leftarrow n + 1$.
 - 11: **until** $r_{n-1} < \epsilon$ or $n \geq N_{\max}$
 - 12: **Output:** Equilibrium mean-field demand $\bar{x}^* \approx \bar{x}^n$ and associated (A, B, \bar{y}) .
-

3.8 Reproducibility and numerical verification

The equilibrium is computed via Algorithm 1 implemented in `code/matlab/mfg_lqg_common_noise_demo.m`. Diagnostics include the fixed-point residual along Picard iterates, a time-step refinement test under decreasing dt , and an N -convergence test comparing particle moments to the mean-field limit.¹

Remark (discrete-time certification). At the discrete-time level, uniqueness of the numerical fixed point can be certified via a Banach fixed-point argument on trajectories endowed with a sup-norm metric. We provide a machine-checkable backbone for this contraction argument in `lean/MFGContraction.lean`; it does not attempt to formalize the full stochastic propagation-of-chaos theorem.

4 Main Results

4.1 Static Benchmark: Price Sensitivity and Overconfidence

The closed-form static price (5) yields explicit comparative statics with respect to overconfidence.

Proposition 4.1 (Static price response increases with overconfidence). *Let $\tau_v = 1/\sigma_v^2$ and $\tau'_\epsilon = k/\sigma_\epsilon^2$. In the static benchmark, the coefficient on v in (5) is*

$$a(k) = \frac{\lambda \tau'_\epsilon}{\gamma + \lambda(\tau_v + \tau'_\epsilon)}, \quad (28)$$

which is increasing in k and satisfies $0 < a(k) < 1$.

4.2 Myopic Trading Rule and Mean-Field Consistency

We next derive a checkable *myopic* trading rule for the dynamic model under (8). Fix an adapted mean-field demand process $\{\bar{x}_t\}_{t \in [0, T]}$ and consider an investor who observes the public price p_t and a private signal ξ_i . For tractability, belief updating (Appendix A) conditions only on the private signal ξ_i ; incorporating the endogenous price as an additional observation channel

¹Outputs and plots can be regenerated by running the script.

would require joint filtering and a richer fixed-point formulation. Conditional on the investor's information, the increment dp_t is Gaussian with conditional variance $\sigma_\eta^2 dt$ and conditional mean $\kappa(\hat{v}_{i,t} - p_t) dt + \lambda\bar{x}_t dt$.

Proposition 4.2 (Myopic CARArule under Gaussian price increments). *Fix $\{\bar{x}_t\}$ and suppose wealth satisfies $dW_{i,t} = x_{i,t} dp_t$. Over an infinitesimal interval, maximizing CARA utility is equivalent to maximizing conditional mean minus $(\gamma/2)$ times conditional variance. The pointwise maximizer is*

$$x_{i,t}^* = \frac{\kappa(\hat{v}_{i,t} - p_t) + \lambda\bar{x}_t}{\gamma\sigma_\eta^2}. \quad (29)$$

Averaging (29) over $i \in [0, 1]$ yields a closed-form *homogeneous* mean-field closure (assuming $\gamma\sigma_\eta^2 > \lambda$):

$$\bar{x}_t = \frac{\kappa}{\gamma\sigma_\eta^2 - \lambda} (m_t - p_t), \quad (48)$$

where $m_t := \int_0^1 \hat{v}_{i,t} di$ is the mean belief. Equations (8) and (48) define a reduced-form equilibrium dynamics in which the feedback loop runs from private signals \rightarrow beliefs \rightarrow demand \rightarrow price.

4.3 Exact continuous-time CARA/LQG control with filtering and mean-field coupling

This subsection replaces the infinitesimal-horizon (myopic) CARA rule with the finite-horizon continuous-time exponential-utility optimum under partial information. We keep the same fundamental/signal/price dynamics (30)–(32) and the same Kalman–Bucy filtering structure for subjective beliefs.

Dynamics and information. Let the fundamental and price evolve as

$$dv_t = \mu_v dt + \sigma_v dW_t, \quad (30)$$

$$d\xi_{i,t} = v_t dt + \sigma_c dU_t + \sigma_\epsilon dB_{i,t}, \quad (31)$$

$$dp_t = \kappa(v_t - p_t) dt + \lambda\bar{x}_t dt + \sigma_\eta dZ_t, \quad (32)$$

where $\bar{x}_t := \int_0^1 x_{j,t} dj$ is the mean-field demand (taken as exogenous by an infinitesimal agent). Agent i observes $(p_s, \xi_{i,s})_{s \leq t}$ and forms a subjective filtered estimate $\hat{v}_{i,t}$.

Subjective Kalman filter (with overconfidence). As in Appendix A, agent i runs a (possibly misspecified) Kalman–Bucy filter

$$\begin{aligned} d\hat{v}_{i,t} &= \mu_v dt + K_t^{(i)}(d\xi_{i,t} - \hat{v}_{i,t} dt), \\ K_t^{(i)} &:= \frac{\Sigma_t^{(i)}}{R'_i}, \quad R'_i := \sigma_c^2 + \frac{\sigma_\epsilon^2}{k_i}, \end{aligned} \quad (33)$$

with Riccati equation

$$\dot{\Sigma}_t^{(i)} = \sigma_v^2 - \frac{(\Sigma_t^{(i)})^2}{R'_i}, \quad \Sigma_0^{(i)} \geq 0. \quad (34)$$

(When convenient, one may use the constant-gain approximation $K_t^{(i)} \approx K_i^\star = \sigma_v / \sqrt{R'_i}$.)

Innovation form and reduced state. Define the (belief-based) mispricing state

$$y_{i,t} := \hat{v}_{i,t} - p_t. \quad (35)$$

Under the agent's filtration, write the observed price in innovations form

$$dp_t = [\kappa y_{i,t} + \lambda \bar{x}_t] dt + \sigma_\eta dI_{i,t}^p, \quad (36)$$

where I_i^p is a Brownian motion (price innovation). Likewise, the (normalized) signal innovation process is defined by

$$dI_{i,t}^\xi := \frac{d\xi_{i,t} - \hat{v}_{i,t} dt}{\sqrt{\sigma_c^2 + \sigma_\epsilon^2}}.$$

Under the agent filtration \mathcal{F}_t^i , I_i^ξ is a Brownian motion and is independent of the price innovation I_i^p .

Consequently, the controlled wealth and the state satisfy

$$dW_{i,t} = x_{i,t} dp_t = x_{i,t} [\kappa y_{i,t} + \lambda \bar{x}_t] dt + x_{i,t} \sigma_\eta dI_{i,t}^p, \quad (37)$$

$$dy_{i,t} = [\mu_v - \kappa y_{i,t} - \lambda \bar{x}_t] dt + \beta_t^{(i)} dI_{i,t}^\xi - \sigma_\eta dI_{i,t}^p, \quad (38)$$

where I_i^ξ is an (independent) Brownian motion and the (subjective) unhedgeable belief-noise loading is

$$\beta_t^{(i)} := K_t^{(i)} \sqrt{\sigma_c^2 + \sigma_\epsilon^2}. \quad (39)$$

Note that $K_t^{(i)}$ depends on the perceived measurement-noise variance $R'_i(k_i)$, whereas the innovation volatility factor $\sqrt{\sigma_c^2 + \sigma_\epsilon^2}$ reflects the true signal-noise variance in $d\xi_{i,t}$.

Equivalently, since $d\xi_{i,t} - \hat{v}_{i,t} dt = \sqrt{\sigma_c^2 + \sigma_\epsilon^2} dI_{i,t}^\xi$, the Kalman–Bucy update (33) can be written in innovation form as

$$d\hat{v}_{i,t} = \mu_v dt + \beta_t^{(i)} dI_{i,t}^\xi.$$

This is the diffusion term that enters the reduced state dynamics (38).

(Under constant gain, $\beta_t^{(i)} \approx \beta_i^* = K_i^* \sqrt{\sigma_c^2 + \sigma_\epsilon^2}$ is constant.)

Diffusions entering the HJB. In the innovation representation (37)–(38), the controlled state is $(W_{i,t}, y_{i,t})$ and is driven by two independent Brownian motions: the *price innovation* I_i^p with volatility σ_η and the *filter innovation* I_i^ξ with volatility $\beta_t^{(i)}$. Consequently, the HJB/Itô generator contains the variance terms $\frac{1}{2} x_{i,t}^2 \sigma_\eta^2 V_{ww}$ and $\frac{1}{2} ((\beta_t^{(i)})^2 + \sigma_\eta^2) V_{yy}$. Moreover, because the same $dI_{i,t}^p$ appears in both $dW_{i,t}$ and $dy_{i,t}$, we have the cross-variation $d\langle W_i, y_i \rangle_t = -x_{i,t} \sigma_\eta^2 dt$, which produces the mixed derivative term $-x_{i,t} \sigma_\eta^2 V_{wy}$ in the HJB and is exactly the source of the intertemporal hedging correction in (46).

Control objective. Agent i maximizes exponential utility of terminal wealth:

$$\sup_{x_i \in \mathcal{A}} \mathbb{E} \left[-\exp(-\gamma_i W_{i,T}) \mid \mathcal{F}_t^i \right], \quad (40)$$

over admissible progressively measurable controls \mathcal{A} with $\mathbb{E} \int_0^T x_{i,t}^2 dt < \infty$.

Exact CARA/LQG solution (finite horizon).

Proposition 4.3 (Exponential-quadratic value and optimal feedback). *Fix a mean-field process $(\bar{x}_t)_{t \in [0, T]}$. The value function admits the exponential-quadratic form*

$$V_i(t, w, y) = -\exp\left(-\gamma_i w - \frac{1}{2} A_t^{(i)} y^2 - B_t^{(i)} y - C_t^{(i)}\right), \quad (41)$$

where $(A_t^{(i)}, B_t^{(i)}, C_t^{(i)})$ solve the backward ODE system with terminal conditions $A_T^{(i)} = B_T^{(i)} = C_T^{(i)} = 0$:

$$-\dot{A}_t^{(i)} = \frac{\kappa^2}{\sigma_\eta^2} - (\beta_t^{(i)})^2 (A_t^{(i)})^2, \quad (42)$$

$$-\dot{B}_t^{(i)} = \frac{\kappa \lambda}{\sigma_\eta^2} \bar{x}_t + \mu_v A_t^{(i)} - (\beta_t^{(i)})^2 A_t^{(i)} B_t^{(i)}, \quad (43)$$

$$-\dot{C}_t^{(i)} = \frac{1}{2} \left(((\beta_t^{(i)})^2 + \sigma_\eta^2) A_t^{(i)} - (\beta_t^{(i)})^2 (B_t^{(i)})^2 \right) \quad (44)$$

$$+ \mu_v B_t^{(i)} + \frac{\lambda^2}{2\sigma_\eta^2} \bar{x}_t^2. \quad (45)$$

The optimal control is the affine feedback

$$x_{i,t}^\star = \frac{\kappa y_{i,t} + \lambda \bar{x}_t}{\gamma_i \sigma_\eta^2} + \frac{A_t^{(i)} y_{i,t} + B_t^{(i)}}{\gamma_i}. \quad (46)$$

The first term is the myopic (instantaneous) demand; the second term is the genuine intertemporal hedging correction induced by the correlation between the state $y_{i,t}$ and traded return noise in (38).

Constant-gain closed form (tight approximation). Under the constant-gain approximation $K_t^{(i)} \approx K_i^\star$ so that $\beta_t^{(i)} \approx \beta_i^\star$ is constant, (42) has the explicit solution

$$\begin{aligned} A_t^{(i)} &\approx \frac{\kappa}{\sigma_\eta \beta_i^\star} \tanh\left(\frac{\kappa \beta_i^\star}{\sigma_\eta} (T - t)\right), \\ \beta_i^\star &:= K_i^\star \sqrt{\sigma_c^2 + \sigma_\epsilon^2}, \\ K_i^\star &:= \frac{\sigma_v}{\sqrt{\sigma_c^2 + \sigma_\epsilon^2/k_i}}. \end{aligned} \quad (47)$$

The remaining $(B_t^{(i)}, C_t^{(i)})$ follow from linear ODEs once \bar{x}_t is specified.

Mean-field consistency (representative-type closure). In a homogeneous population (single type) with coefficients (γ, k) and hence common continuous-time coefficients $(A_t^{\text{ct}}, B_t^{\text{ct}})$, taking cross-sectional means of (46) yields

$$\bar{x}_t = \frac{(\kappa + \sigma_\eta^2 A_t^{\text{ct}}) \bar{y}_t + \sigma_\eta^2 B_t^{\text{ct}}}{\gamma \sigma_\eta^2 - \lambda}, \quad (48)$$

where $\bar{y}_t := \int_0^1 y_{i,t} di = m_t - p_t$. which reduces to Proposition 4.2 when $(A_t^{\text{ct}}, B_t^{\text{ct}}) \equiv (0, 0)$. In regimes where symmetry/centering implies $B_t^{\text{ct}} \equiv 0$ (e.g. $\mu_v = 0$ and no exogenous bias), the equilibrium amplification is governed by the single scalar coefficient $\kappa + \sigma_\eta^2 A_t^{\text{ct}}$ in (48).

4.4 Level Amplification vs. Overconfidence Effects

The baseline calibration intentionally uses strong anchoring ($\kappa = 0.005$) and moderate impact ($\lambda = 0.20$), resulting in modest overconfidence effects on mispricing ($|\Delta\mathbb{E}[|p - v|]| \approx 0.004$). This subsection distinguishes two notions: (i) *level amplification*—large mispricing/volatility levels driven by weak anchoring and/or high noise trading; and (ii) *overconfidence (treatment) effects*—incremental differences when increasing k from 1 to 3. The numerical results (Section 6.3) show substantial level amplification under stress regimes, while k -effects on mispricing remain modest across parameterizations. The following proposition gives an analytical mechanism for why k predominantly affects disagreement rather than mispricing.

Proposition 4.4 (Mechanism: mean-belief closure and why k shifts dispersion more than price). *Within the myopic mean-field equilibrium (homogeneous closure (48)):*

- (i) **Closure depends only on the mean belief.** The equilibrium demand \bar{x}_t and hence the price dynamics (8) depend on the belief distribution only through $m_t - p_t$, where $m_t := \int_0^1 \hat{v}_{i,t} di$ is the cross-sectional mean belief (Section III and (20)). In particular, cross-sectional variance (disagreement) does not enter the mean-field fixed point.
- (ii) **Decomposition of mispricing.** Let $y_t := p_t - v_t$ (mispricing) and $e_t := m_t - v_t$ (mean-belief tracking error). Under the constant-gain approximation, the pair (y_t, e_t) satisfies the linear system (59): mispricing dynamics are driven by (a) microstructure regime $(\kappa, \lambda, \sigma_\eta)$ through the coefficient $c := \lambda\kappa/(\gamma\sigma_\eta^2 - \lambda)$ and the mean-reversion rate $\kappa + c$; and (b) the mean-belief term e_t , which is the only channel through which the belief distribution affects price. Thus $\mathbb{E}[|p - v|]$ and stationary mispricing variance are determined by $(\kappa, \lambda, \sigma_\eta)$ and the stationary law of e_t .
- (iii) **Why k predominantly affects disagreement.** Under the information structure of Appendix A, each agent's belief has a common component (loading $K^*(k)\sigma_c$ on dU_t) and an idiosyncratic component (loading $K^*(k)\sigma_\epsilon$ on $dB_{i,t}$). The cross-sectional mean m_t aggregates beliefs, so the idiosyncratic components average out and m_t is driven only by the common noise and the fundamental. By Proposition 4.8, disagreement $D_\infty(k) = \text{Var}(\hat{v}_{i,t} - m_t \mid \mathcal{F}^0)$ is strictly increasing in k . By Proposition 4.9, the mean-belief error $e_t = m_t - v_t$ has stationary variance $\text{Var}(e_\infty)$ that depends on k only through $K^*(k)$ and need not be monotone in k (common-noise and fundamental-noise terms enter with opposite scaling in $1/K^*$). Hence incremental increases in k raise cross-sectional variance (disagreement) and trading intensity by construction, while the mean belief—and therefore equilibrium demand and mispricing—respond only weakly because they depend on e_t , whose variance is bounded and not uniformly amplified in k .

Level amplification from market microstructure. Weak anchoring ($\kappa < 0.002$) and/or high noise trading ($\sigma_\eta > 0.75$) can generate large mispricing and volatility levels (e.g., $\mathbb{E}[|p - v|]$ exceeding 3–9 vs. ≈ 1.9 in baseline). This level amplification is primarily driven by (κ, σ_η) rather than the overconfidence parameter k : within stress cases, outcomes are nearly unchanged between $k = 1$ and $k = 3$ (Table 14).

Overconfidence effects: primarily on disagreement and trading intensity. In both baseline and stress calibrations, increasing k from 1 to 3 primarily increases cross-sectional disagreement ($\Delta\mathbb{E}[\sigma_i(\hat{v}_i)] \approx +0.059$) and trading intensity, while effects on mispricing levels remain modest ($|\Delta\mathbb{E}[|p - v|]| \approx 0.004$ in baseline, similarly small in stress cases). Proposition 4.4 provides the analytical reason: the mean-field closure depends only on the mean belief, so k inflates

dispersion (and thus trading intensity) more than the mean belief, and hence mispricing responds only weakly.

Structural extensions (potential mechanisms). The model can be extended with structural mechanisms that could amplify mispricing persistence or volatility: (i) *State-dependent anchoring*: $\kappa(t) = \kappa_{\text{base}} \exp(-\alpha_\kappa |p_t - v_t|)$ weakens arbitrage pressure under extreme mispricing (limits to arbitrage); (ii) *Endogenous fundamental feedback*: $dv_t = \mu_v dt + \sigma_v dW_t + \beta_{\text{feedback}}(p_t - v_t) dt$ creates reflexive price–fundamental loops; (iii) *Overconfidence-dependent impact*: $\lambda_{\text{eff}} = \lambda_{\text{base}}(1 + \beta_\lambda(\bar{k}_t - 1))$ makes impact increase with aggregate overconfidence. These extensions are implemented in the codebase (Section 6.3) but are not the focus of the current numerical results, which demonstrate level amplification from (κ, σ_η) rather than k -driven amplification.

Scope and interpretation. Proposition 4.3 relies on our price-taking mean-field specification and on the simplification that belief updating conditions only on the private signal (Appendix A). In the particle simulations we implement a discrete-time mean-field consistent dynamics: at each step we compute \bar{x}_t as the finite- N fixed point of the linear system induced by (29) with an effective risk term that includes belief uncertainty. Equation (48) is presented as a transparent homogeneous benchmark and provides a stability condition for the closed-loop linear dynamics (see Proposition 4.7).

Proposition 4.5 (Per-step fixed point in the particle implementation). *In the discrete-time particle implementation, we use an effective variance*

$$\text{Var}_{i,t}^{\text{eff}} := \sigma_\eta^2 + \kappa^2 \Sigma_{i,t} \Delta t, \quad (49)$$

and the myopic rule takes the linear form

$$x_{i,t} = \frac{\alpha_0}{\gamma \text{Var}_{i,t}^{\text{eff}}} \left(\kappa(\hat{v}_{i,t} - p_t) + \lambda \bar{x}_t \right). \quad (50)$$

This form follows by applying the mean-variance argument behind Proposition 4.2 to the Euler increment $\Delta p_{t+1} := p_{t+1} - p_t = \kappa(v_t - p_t)\Delta t + \lambda \bar{x}_t \Delta t + \sigma_\eta \sqrt{\Delta t} \varepsilon_{t+1}^\eta$: conditional on \mathcal{F}_t^i , the drift depends on $\hat{v}_{i,t}$ and the variance satisfies $\text{Var}_{i,t}(\Delta p_{t+1}) = \sigma_\eta^2 \Delta t + \kappa^2 \Sigma_{i,t}(\Delta t)^2$, hence the optimal one-step demand depends on the “variance per unit time” $\sigma_\eta^2 + \kappa^2 \Sigma_{i,t} \Delta t$. The scalar $\alpha_0 > 0$ is an optional position-size (risk-budget) scaling (set to $\alpha_0 = 1$ in our baseline) and can be absorbed into a rescaling of γ . Define $A_t := \frac{1}{N} \sum_{i=1}^N \frac{\alpha_0 \kappa(\hat{v}_{i,t} - p_t)}{\gamma \text{Var}_{i,t}^{\text{eff}}}$ and $B_t := \frac{1}{N} \sum_{i=1}^N \frac{\alpha_0 \lambda}{\gamma \text{Var}_{i,t}^{\text{eff}}}$. If $1 - B_t > 0$, the scalar fixed point $\bar{x}_t = \frac{1}{N} \sum_i x_{i,t}$ exists and is unique and is given by

$$\bar{x}_t = \frac{A_t}{1 - B_t}. \quad (51)$$

Theorem 4.6 (Contraction and uniqueness of the per-step mean-field closure). *Fix time t and treat the belief states $(\hat{v}_{i,t}, \Sigma_{i,t})$ and the public price p_t as given. Define the affine mean-field map*

$$\Phi_t(\bar{x}) := \frac{1}{N} \sum_{i=1}^N x_{i,t}(\bar{x}) = A_t + B_t \bar{x}, \quad (52)$$

where A_t, B_t are as in Proposition 4.5. If $0 \leq B_t < 1$, then Φ_t is a contraction on \mathbb{R} with constant B_t and has a unique fixed point $\bar{x}_t = A_t/(1 - B_t)$. Moreover, since $\text{Var}_{i,t}^{\text{eff}} \geq \sigma_\eta^2$, a simple sufficient condition ensuring $B_t < 1$ uniformly is

$$\frac{\alpha_0 \lambda}{\gamma \sigma_\eta^2} < 1. \quad (53)$$

Proposition 4.7 (Closed-loop stability in a homogeneous benchmark). *Assume the homogeneous closure (48) holds and, for this benchmark calculation, that the mean belief tracks the fundamental ($m_t = v_t$). Then the mispricing $y_t := p_t - v_t$ satisfies the linear SDE*

$$\begin{aligned} dy_t &= -\kappa_{\text{eff}} y_t dt - \mu_v dt + \sigma_\eta dZ_t - \sigma_v dW_t, \\ \kappa_{\text{eff}} &:= \kappa \frac{\gamma\sigma_\eta^2}{\gamma\sigma_\eta^2 - \lambda}. \end{aligned} \tag{54}$$

In particular, if $\gamma\sigma_\eta^2 > \lambda$ then $\kappa_{\text{eff}} > 0$ and y_t is mean-reverting (Ornstein–Uhlenbeck). If additionally $\mu_v = 0$, the stationary variance is $\text{Var}(y_\infty) = (\sigma_\eta^2 + \sigma_v^2)/(2\kappa_{\text{eff}})$.

4.5 Uniqueness and Stability Conditions (Multiplicity and Blow-Ups)

The following conditions rule out multiple equilibria and blow-ups. **Continuous-time LQG map** Φ (Section 3.7): if $\gamma\sigma_\eta^2 > \lambda$ (positive denominator, well-posedness) and $q < 1$, then Φ is a contraction on $(\mathcal{X}, \|\cdot\|_\infty)$, so the fixed point is unique and Picard iteration does not blow up (see Proposition 3.7). **Discrete-time per-step:** if $1 - B_t > 0$, the scalar fixed point $\bar{x}_t = A_t/(1 - B_t)$ is unique; a sufficient condition is $\alpha_0\lambda/(\gamma\sigma_\eta^2) < 1$ (see Theorem 4.6 and Proposition 4.5). **Closed-loop paths (mispricing):** if $\gamma\sigma_\eta^2 > \lambda$, then $\kappa_{\text{eff}} > 0$ and mispricing y_t is mean-reverting, so y_t does not explode (see Proposition 4.7). **Black-box MFG limit:** under (H1)–(H5), the equilibrium flow is unique and $\bar{\mu}_t^N$ converges to μ_t at rate $O(1/N)$ (see Proposition 3.5 in the mean-field limit subsection).

4.6 Option B: Stationary Moments With Explicit k -Dependence

Proposition 4.7 provides a transparent OU benchmark for mispricing, but it removes the overconfidence channel by imposing $m_t = v_t$. We now record complementary stationary-moment calculations in which k enters explicitly through the steady-state filtering gain (Appendix A). Lemma A.1 shows that the perceived Riccati equation converges exponentially to the steady state, motivating the constant-gain approximation used below (interpretable as an asymptotic stationary regime after burn-in).

Proposition 4.8 (Stationary disagreement and monotonicity in k (constant-gain approximation)). *Assume a homogeneous overconfidence type k and approximate the Kalman–Bucy gain by its steady-state value $K^*(k) = \sigma_v/\sqrt{R'(k)}$, where $R'(k) = \sigma_c^2 + \sigma_\epsilon^2/k$ (Appendix A). Let $m_t := \int_0^1 \hat{v}_{i,t} di$ and define the cross-sectional deviation $\delta_{i,t} := \hat{v}_{i,t} - m_t$. Conditioning on the common filtration \mathcal{F}_t^0 , the deviations satisfy the OU dynamics*

$$d\delta_{i,t} = -K^*(k) \delta_{i,t} dt + K^*(k) \sigma_\epsilon dB_{i,t}. \tag{55}$$

Consequently, the conditional disagreement $D_t := \text{Var}(\hat{v}_{i,t} \mid \mathcal{F}_t^0) = \text{Var}(\delta_{i,t} \mid \mathcal{F}_t^0)$ admits the stationary value

$$D_\infty(k) = \frac{K^*(k)\sigma_\epsilon^2}{2} = \frac{\sigma_v\sigma_\epsilon^2}{2\sqrt{\sigma_c^2 + \sigma_\epsilon^2/k}}, \tag{56}$$

which is strictly increasing in k .

Proposition 4.9 (Stationary mean-belief tracking error (constant-gain approximation)). *Under the same constant-gain approximation, define the mean-belief tracking error $e_t := m_t - v_t$. Then*

$$de_t = -K^*(k) e_t dt + K^*(k) \sigma_c dU_t - \sigma_v dW_t, \tag{57}$$

and the stationary variance is

$$\text{Var}(e_\infty) = \frac{(K^*(k))^2 \sigma_c^2 + \sigma_v^2}{2K^*(k)} = \frac{K^*(k)\sigma_c^2}{2} + \frac{\sigma_v^2}{2K^*(k)}. \quad (58)$$

In particular, k enters the stationary tracking quality through $K^*(k)$ and can generate a trade-off (not necessarily monotone in k).

Proposition 4.10 (Stationary mispricing with belief feedback (2D OU / Lyapunov form)). *Assume $\mu_v = 0$ and use the homogeneous closure (48). Under the constant-gain approximation above, the pair (y_t, e_t) with $y_t := p_t - v_t$ satisfies the linear system*

$$\begin{aligned} dy_t &= -(\kappa + c)y_t dt + c e_t dt + \sigma_\eta dZ_t - \sigma_v dW_t, \\ de_t &= -K^*(k)e_t dt + K^*(k)\sigma_c dU_t - \sigma_v dW_t, \end{aligned} \quad (59)$$

where $c := \lambda\kappa/(\gamma\sigma_\eta^2 - \lambda)$. If $\gamma\sigma_\eta^2 > \lambda$ and $K^*(k) > 0$, then the drift matrix

$$A(k) := \begin{bmatrix} -(\kappa + c) & c \\ 0 & -K^*(k) \end{bmatrix}$$

is Hurwitz and the stationary covariance $P(k) = \mathbb{E}[X_\infty X_\infty^\top]$ for $X_t = (y_t, e_t)$ is the unique solution of the Lyapunov equation

$$A(k)P(k) + P(k)A(k)^\top + Q(k) = 0, \quad (60)$$

where $Q(k)$ is the diffusion covariance implied by (59). Thus $\text{Var}(y_\infty)$ depends on k explicitly through $K^*(k)$.

Corollary 4.11 (Closed-form stationary variances for Proposition 4.10). *In the setting of Proposition 4.10, write $K := K^*(k)$ and define the noise covariances $q_{11} := \sigma_\eta^2 + \sigma_v^2$, $q_{12} := \sigma_v^2$, and $q_{22} := K^2\sigma_c^2 + \sigma_v^2$. Then the Lyapunov equation (60) has the explicit solution $P = \begin{pmatrix} p_{11} & p_{12} \\ p_{12} & p_{22} \end{pmatrix}$ with*

$$\begin{aligned} p_{22} &= \frac{q_{22}}{2K} = \frac{K\sigma_c^2}{2} + \frac{\sigma_v^2}{2K}, \\ p_{12} &= \frac{cp_{22} + q_{12}}{\kappa + c + K}, \\ p_{11} &= \frac{cp_{12} + q_{11}/2}{\kappa + c}. \end{aligned} \quad (61)$$

In particular, $\text{Var}(y_\infty) = p_{11}$ depends on k through $K^*(k)$.

4.7 Connection to Numerical Results

Section VI simulates a large- N particle system implementing (8), Kalman belief updates (Appendix A), and the feedback policy (29) (implemented in discrete time with an effective variance that includes belief uncertainty). Overconfidence enters only through belief updating (misperceived signal precision), and we report price/mispricing/volatility statistics across bull/bear drifts μ_v and overconfidence levels k .

5 PROOFS

Proof of Proposition 4.1

Proof. From the static price equation (5), the coefficient on v is

$$a(k) = \frac{\lambda\tau'_\epsilon}{\gamma + \lambda(\tau_v + \tau'_\epsilon)}, \quad \tau'_\epsilon = \frac{k}{\sigma_\epsilon^2}, \quad \tau_v = \frac{1}{\sigma_v^2}.$$

Set $u := \tau'_\epsilon > 0$ and define $f(u) := \frac{\lambda u}{\gamma + \lambda(\tau_v + u)}$. Then $a(k) = f(\tau'_\epsilon)$ and

$$f'(u) = \frac{\lambda(\gamma + \lambda\tau_v)}{(\gamma + \lambda(\tau_v + u))^2} > 0,$$

so f is strictly increasing in u , hence $a(k)$ is strictly increasing in k . Moreover, $a(k) > 0$ is immediate since all parameters are positive, and

$$a(k) < 1 \iff \lambda u < \gamma + \lambda(\tau_v + u) \iff 0 < \gamma + \lambda\tau_v,$$

which holds. Thus $0 < a(k) < 1$ and $a(k)$ increases with k . \square

Proof of Proposition 4.2

Proof. Fix an adapted mean-field demand $\{\bar{x}_t\}$ and consider the price dynamics (8):

$$dp_t = \kappa(v_t - p_t) dt + \lambda\bar{x}_t dt + \sigma_\eta dZ_t.$$

In this proposition we condition on the investor's information \mathcal{F}_t^i and use the modeling simplification stated in the paper: the investor's conditional mean for v_t is $\hat{v}_{i,t}$, so the investor's conditional drift for p is

$$\mu_{p,i}(t) := \mathbb{E}[dp_t | \mathcal{F}_t^i]/dt = \kappa(\hat{v}_{i,t} - p_t) + \lambda\bar{x}_t,$$

and the conditional variance rate is $\text{Var}(dp_t | \mathcal{F}_t^i)/dt = \sigma_\eta^2$.

Wealth follows $dW_{i,t} = x_{i,t} dp_t$. Over an infinitesimal interval $[t, t + dt]$, the increment $\Delta W_{i,t} := W_{i,t+dt} - W_{i,t} = x_{i,t} dp_t$ is Gaussian conditional on \mathcal{F}_t^i with

$$\begin{aligned} \mathbb{E}[\Delta W_{i,t} | \mathcal{F}_t^i] &= x_{i,t}\mu_{p,i}(t) dt, \\ \text{Var}(\Delta W_{i,t} | \mathcal{F}_t^i) &= x_{i,t}^2\sigma_\eta^2 dt. \end{aligned}$$

For CARA utility $U(w) = -e^{-\gamma w}$ and conditional Gaussian ΔW , we have the standard identity: if $X \sim N(m, s^2)$ then

$$\mathbb{E}[-e^{-\gamma X}] = -\exp\left(-\gamma m + \frac{\gamma^2}{2}s^2\right).$$

Applying this with $X = W_{i,t} + \Delta W_{i,t}$ (where $W_{i,t}$ is \mathcal{F}_t^i -measurable), maximizing $\mathbb{E}[-e^{-\gamma(W_{i,t} + \Delta W_{i,t})} | \mathcal{F}_t^i]$ over $x_{i,t}$ is equivalent to maximizing (up to the common factor $dt > 0$) the concave quadratic

$$x_{i,t}\mu_{p,i}(t) - \frac{\gamma}{2}x_{i,t}^2\sigma_\eta^2.$$

The first-order condition is $\mu_{p,i}(t) - \gamma\sigma_\eta^2 x_{i,t} = 0$, giving

$$x_{i,t}^* = \frac{\mu_{p,i}(t)}{\gamma\sigma_\eta^2} = \frac{\kappa(\hat{v}_{i,t} - p_t) + \lambda\bar{x}_t}{\gamma\sigma_\eta^2},$$

which is (29).

For the mean-field closure, average (29) over $i \in [0, 1]$:

$$\bar{x}_t = \frac{\kappa(m_t - p_t) + \lambda\bar{x}_t}{\gamma\sigma_\eta^2}, \quad m_t := \int_0^1 \hat{v}_{i,t} di.$$

Rearranging yields $(\gamma\sigma_\eta^2 - \lambda)\bar{x}_t = \kappa(m_t - p_t)$, so if $\gamma\sigma_\eta^2 > \lambda$ then

$$\bar{x}_t = \frac{\kappa}{\gamma\sigma_\eta^2 - \lambda}(m_t - p_t),$$

which is (48). \square

Proof of Proposition 4.5

Proof. Work on the discrete grid with step Δt and the Euler increment

$$\begin{aligned} \Delta p_{t+1} := p_{t+1} - p_t &= \kappa(v_t - p_t)\Delta t + \lambda\bar{x}_t\Delta t \\ &\quad + \sigma_\eta\sqrt{\Delta t}\varepsilon_{t+1}^\eta, \\ \varepsilon_{t+1}^\eta &\sim N(0, 1). \end{aligned}$$

Conditional on investor i 's information \mathcal{F}_t^i , we have $\mathbb{E}[v_t | \mathcal{F}_t^i] = \hat{v}_{i,t}$ and $\text{Var}(v_t | \mathcal{F}_t^i) = \Sigma_{i,t}$. Hence

$$\mathbb{E}[\Delta p_{t+1} | \mathcal{F}_t^i] = (\kappa(\hat{v}_{i,t} - p_t) + \lambda\bar{x}_t)\Delta t,$$

and, using independence of ε_{t+1}^η from \mathcal{F}_t^i and from v_t ,

$$\begin{aligned} \text{Var}(\Delta p_{t+1} | \mathcal{F}_t^i) &= \kappa^2 \text{Var}(v_t | \mathcal{F}_t^i)(\Delta t)^2 + \sigma_\eta^2\Delta t \\ &= \kappa^2\Sigma_{i,t}(\Delta t)^2 + \sigma_\eta^2\Delta t. \end{aligned}$$

Under the per-step myopic mean-variance approximation (the discrete analogue of Proposition 4.2), the investor chooses $x_{i,t}$ to maximize

$$x_{i,t} \mathbb{E}[\Delta p_{t+1} | \mathcal{F}_t^i] - \frac{\gamma}{2}x_{i,t}^2 \text{Var}(\Delta p_{t+1} | \mathcal{F}_t^i).$$

Substituting the conditional moments above and dividing by the common factor $\Delta t > 0$ gives the equivalent problem

$$\max_{x_{i,t}} x_{i,t}(\kappa(\hat{v}_{i,t} - p_t) + \lambda\bar{x}_t) - \frac{\gamma}{2}x_{i,t}^2(\sigma_\eta^2 + \kappa^2\Sigma_{i,t}\Delta t).$$

The unique maximizer is

$$x_{i,t}^* = \frac{\kappa(\hat{v}_{i,t} - p_t) + \lambda\bar{x}_t}{\gamma(\sigma_\eta^2 + \kappa^2\Sigma_{i,t}\Delta t)}.$$

Including the optional scale $\alpha_0 > 0$ (risk-budget/position-size parameter) yields (50) with

$$\text{Var}_{i,t}^{\text{eff}} := \sigma_\eta^2 + \kappa^2\Sigma_{i,t}\Delta t,$$

Write (50) as $x_{i,t} = a_{i,t} + b_{i,t}\bar{x}_t$ with

$$a_{i,t} := \frac{\alpha_0\kappa(\hat{v}_{i,t} - p_t)}{\gamma\text{Var}_{i,t}^{\text{eff}}}, \quad b_{i,t} := \frac{\alpha_0\lambda}{\gamma\text{Var}_{i,t}^{\text{eff}}}.$$

Averaging over $i = 1, \dots, N$ gives $\bar{x}_t = A_t + B_t\bar{x}_t$ where A_t, B_t are as defined in the paper, hence $(1 - B_t)\bar{x}_t = A_t$. If $1 - B_t > 0$ the unique solution is $\bar{x}_t = A_t/(1 - B_t)$, as claimed. \square

Proof of Theorem 4.6

Proof. By Proposition 4.5, for fixed $(\hat{v}_{i,t}, \Sigma_{i,t})_{i=1}^N$ and p_t , the per-step map is affine:

$$\Phi_t(\bar{x}) = \frac{1}{N} \sum_{i=1}^N x_{i,t}(\bar{x}) = A_t + B_t \bar{x}.$$

For any \bar{x}, \bar{x}' ,

$$|\Phi_t(\bar{x}) - \Phi_t(\bar{x}')| = |B_t| |\bar{x} - \bar{x}'|.$$

Thus if $0 \leq B_t < 1$, Φ_t is a contraction on \mathbb{R} with contraction constant B_t and has a unique fixed point, which must satisfy $\bar{x} = \Phi_t(\bar{x}) = A_t + B_t \bar{x}$, i.e. $\bar{x} = A_t/(1 - B_t)$.

For the sufficient uniform condition: since $\Sigma_{i,t} \geq 0$ and $\Delta t > 0$, we have $\text{Var}_{i,t}^{\text{eff}} = \sigma_\eta^2 + \kappa^2 \Sigma_{i,t} \Delta t \geq \sigma_\eta^2$, hence

$$B_t = \frac{1}{N} \sum_{i=1}^N \frac{\alpha_0 \lambda}{\gamma \text{Var}_{i,t}^{\text{eff}}} \leq \frac{1}{N} \sum_{i=1}^N \frac{\alpha_0 \lambda}{\gamma \sigma_\eta^2} = \frac{\alpha_0 \lambda}{\gamma \sigma_\eta^2}.$$

Therefore $\alpha_0 \lambda / (\gamma \sigma_\eta^2) < 1$ implies $B_t < 1$ for all t . \square

Proof of Theorem 3.1 (Well-posedness of the discrete-time particle system)

Proof. Fix $T \in \mathbb{N}$, $\Delta t > 0$, and fix a realization of all common and idiosyncratic shock sequences used by the algorithm. We show by induction on $t = 0, 1, \dots, T$ that the state

$$S_t = (v_t, p_t, \{(\hat{v}_{i,t}, \Sigma_{i,t})\}_{i=1}^N, \bar{x}_t)$$

is uniquely determined and adapted.

At $t = 0$, $(v_0, p_0, \{\hat{v}_{i,0}, \Sigma_{i,0}\}_{i=1}^N)$ are given by assumption (A1). Suppose the system is uniquely defined up to time t . Then:

1. By (A2), the discrete-time Kalman recursion in Appendix A defines each $(\hat{v}_{i,t}, \Sigma_{i,t})$ uniquely from $(\hat{v}_{i,t-1}, \Sigma_{i,t-1})$ and the realized private signal at time t (which is a measurable function of the fixed shock sequences and v_t).
2. Given $(\hat{v}_{i,t}, \Sigma_{i,t})_{i=1}^N$ and p_t , the per-step demand map Φ_t is well-defined by Proposition 4.5. By (A3) (e.g. $B_t < 1$), Φ_t has a unique fixed point \bar{x}_t , and then each $x_{i,t}$ is uniquely determined.
3. Finally, by (A4), the Euler updates for v_{t+1} and p_{t+1} are explicit measurable functions of (v_t, p_t) , \bar{x}_t , and the realized shocks at time $t + 1$, hence define unique (v_{t+1}, p_{t+1}) .

Thus S_{t+1} is uniquely determined from S_t and the fixed shocks, and is adapted to the natural filtration generated by the shocks. Induction completes the proof, yielding a unique adapted solution path on $\{0, 1, \dots, T\}$. \square

Proof of Proposition 4.8 (Constant-gain approximation)

Proof. Assume a homogeneous type k and adopt the constant-gain approximation $K_t \equiv K^*(k) =: K > 0$. From Appendix A, the (subjective) Kalman–Bucy filter is

$$d\hat{v}_{i,t} = \mu_v dt + K(d\xi_{i,t} - \hat{v}_{i,t} dt).$$

Using the observation equation (31),

$$d\xi_{i,t} = v_t dt + \sigma_c dU_t + \sigma_\epsilon dB_{i,t},$$

so substituting gives

$$\begin{aligned} d\hat{v}_{i,t} &= \mu_v dt + K((v_t - \hat{v}_{i,t}) dt + \sigma_c dU_t + \sigma_\epsilon dB_{i,t}) \\ &= (\mu_v + K(v_t - \hat{v}_{i,t})) dt + K\sigma_c dU_t + K\sigma_\epsilon dB_{i,t}. \end{aligned}$$

Let $m_t := \int_0^1 \hat{v}_{i,t} di$ be the cross-sectional mean belief. Under a continuum (or large- N) approximation, the idiosyncratic noises average out, i.e. $\int_0^1 dB_{i,t} di = 0$ in the sense of laws/LLN, while the common term U_t persists. Averaging the SDE over i yields

$$dm_t = (\mu_v + K(v_t - m_t)) dt + K\sigma_c dU_t.$$

Define the deviation $\delta_{i,t} := \hat{v}_{i,t} - m_t$. Subtracting the m_t equation from the $\hat{v}_{i,t}$ equation cancels the common-noise terms and gives

$$\begin{aligned} d\delta_{i,t} &= -K(\hat{v}_{i,t} - m_t) dt + K\sigma_\epsilon dB_{i,t} \\ &= -K\delta_{i,t} dt + K\sigma_\epsilon dB_{i,t}, \end{aligned}$$

which is (55).

Now condition on the common filtration $\mathcal{F}_t^0 := \sigma(W_s, U_s, Z_s : s \leq t)$. Conditional on \mathcal{F}_t^0 , $\delta_{i,t}$ solves an OU SDE driven only by the idiosyncratic Brownian motion $B_{i,t}$, so its conditional variance $D_t := \text{Var}(\delta_{i,t} | \mathcal{F}_t^0) = \mathbb{E}[\delta_{i,t}^2 | \mathcal{F}_t^0]$ satisfies (Itô + tower property)

$$\begin{aligned} d(\delta_{i,t}^2) &= 2\delta_{i,t} d\delta_{i,t} + (d\delta_{i,t})^2 \\ &= (-2K\delta_{i,t}^2 + K^2\sigma_\epsilon^2) dt + 2K\sigma_\epsilon\delta_{i,t} dB_{i,t}. \end{aligned}$$

Taking \mathcal{F}_t^0 -conditional expectation kills the martingale term and yields the linear ODE

$$\frac{d}{dt}D_t = -2KD_t + K^2\sigma_\epsilon^2.$$

Hence $D_t \rightarrow D_\infty := \frac{K^2\sigma_\epsilon^2}{2K} = \frac{K\sigma_\epsilon^2}{2}$, giving (56).

Finally, with $R'(k) = \sigma_c^2 + \sigma_\epsilon^2/k$ we have $K^*(k) = \sigma_v/\sqrt{R'(k)}$, which is strictly increasing in k because $R'(k)$ is strictly decreasing in k ; therefore $D_\infty(k) = (K^*(k)\sigma_\epsilon^2)/2$ is strictly increasing in k . \square

Proof of Proposition 4.9 (Constant-gain approximation)

Proof. Under the constant-gain approximation (same setting as Proposition 4.8), we derived

$$dm_t = (\mu_v + K(v_t - m_t)) dt + K\sigma_c dU_t.$$

The fundamental satisfies $dv_t = \mu_v dt + \sigma_v dW_t$. Define $e_t := m_t - v_t$. Then

$$\begin{aligned} de_t &= dm_t - dv_t \\ &= (\mu_v + K(v_t - m_t)) dt + K\sigma_c dU_t - \mu_v dt - \sigma_v dW_t \\ &= -Ke_t dt + K\sigma_c dU_t - \sigma_v dW_t, \end{aligned}$$

which is (57).

Since U and W are independent Brownian motions, e_t is an OU process with mean-reversion rate K and diffusion variance rate $K^2\sigma_c^2 + \sigma_v^2$. The stationary variance is the standard OU value

$$\text{Var}(e_\infty) = \frac{K^2\sigma_c^2 + \sigma_v^2}{2K} = \frac{K\sigma_c^2}{2} + \frac{\sigma_v^2}{2K},$$

which is (58). \square

Proof of Proposition 4.10 (2D OU / Lyapunov form)

Proof. Assume $\mu_v = 0$ and the homogeneous closure (48):

$$\bar{x}_t = \frac{\kappa}{\gamma\sigma_\eta^2 - \lambda}(m_t - p_t).$$

Write $y_t := p_t - v_t$ and $e_t := m_t - v_t$. Using $m_t - p_t = (m_t - v_t) - (p_t - v_t) = e_t - y_t$, the price SDE (8) becomes

$$\begin{aligned} dp_t &= \kappa(v_t - p_t) dt + \lambda\bar{x}_t dt + \sigma_\eta dZ_t \\ &= -\kappa y_t dt + \frac{\lambda\kappa}{\gamma\sigma_\eta^2 - \lambda}(e_t - y_t) dt + \sigma_\eta dZ_t. \end{aligned}$$

Let $c := \lambda\kappa/(\gamma\sigma_\eta^2 - \lambda)$. Then

$$dp_t = -(\kappa + c)y_t dt + ce_t dt + \sigma_\eta dZ_t.$$

Since $\mu_v = 0$, $dv_t = \sigma_v dW_t$, hence

$$dy_t = dp_t - dv_t = -(\kappa + c)y_t dt + ce_t dt + \sigma_\eta dZ_t - \sigma_v dW_t.$$

From Proposition 4.9, the mean-belief tracking error satisfies

$$de_t = -Ke_t dt + K\sigma_c dU_t - \sigma_v dW_t, \quad K := K^*(k) > 0.$$

Stacking $X_t = (y_t, e_t)^\top$ yields the linear system (59) with drift matrix

$$A(k) = \begin{pmatrix} -(\kappa + c) & c \\ 0 & -K \end{pmatrix}$$

and diffusion matrix $G(k)$ as stated.

If $\gamma\sigma_\eta^2 > \lambda$ then $c > 0$ and $\kappa + c > 0$; also $K > 0$ by definition. The eigenvalues of $A(k)$ are $-(\kappa + c)$ and $-K$, hence strictly negative: $A(k)$ is Hurwitz. For a Hurwitz A , the continuous-time Lyapunov equation

$$AP + PA^\top + GG^\top = 0$$

has a unique symmetric positive semidefinite solution P , which equals the stationary covariance $P = \mathbb{E}[X_\infty X_\infty^\top]$. This gives (60) and shows $\text{Var}(y_\infty)$ depends on k through $K^*(k)$. \square

Proof of Corollary 4.11 (Closed-form stationary variances)

Proof. Let $A = \begin{pmatrix} -(\kappa + c) & c \\ 0 & -K \end{pmatrix}$ and $Q := GG^\top$. Because dZ_t, dU_t, dW_t are independent, from (59) we have

$$Q = \begin{pmatrix} \sigma_\eta^2 + \sigma_v^2 & \sigma_v^2 \\ \sigma_v^2 & K^2\sigma_c^2 + \sigma_v^2 \end{pmatrix} =: \begin{pmatrix} q_{11} & q_{12} \\ q_{12} & q_{22} \end{pmatrix}.$$

Write $P = \begin{pmatrix} p_{11} & p_{12} \\ p_{12} & p_{22} \end{pmatrix}$. Compute

$$\begin{aligned} AP &= \begin{pmatrix} -(\kappa + c)p_{11} + cp_{12} & -(\kappa + c)p_{12} + cp_{22} \\ -Kp_{12} & -Kp_{22} \end{pmatrix}, \\ PA^\top &= \begin{pmatrix} -(\kappa + c)p_{11} + cp_{12} & -Kp_{12} \\ -(\kappa + c)p_{12} + cp_{22} & -Kp_{22} \end{pmatrix}. \end{aligned}$$

Thus the Lyapunov equation $AP + PA^\top + Q = 0$ yields the entrywise system:

$$\begin{aligned} (2, 2) : & -2Kp_{22} + q_{22} = 0, \\ (1, 2) : & -(\kappa + c + K)p_{12} + cp_{22} + q_{12} = 0, \\ (1, 1) : & -2(\kappa + c)p_{11} + 2cp_{12} + q_{11} = 0. \end{aligned}$$

Solving sequentially gives

$$\begin{aligned} p_{22} &= \frac{q_{22}}{2K} = \frac{K^2\sigma_c^2 + \sigma_v^2}{2K} = \frac{K\sigma_c^2}{2} + \frac{\sigma_v^2}{2K}, \\ p_{12} &= \frac{cp_{22} + q_{12}}{\kappa + c + K}, \quad p_{11} = \frac{cp_{12} + q_{11}/2}{\kappa + c}, \end{aligned}$$

which matches the closed-form expressions in Corollary 4.11. \square

Proof of Proposition 4.7 (Homogeneous closed-loop stability benchmark)

Proof. Assume the homogeneous closure (48) holds and, for this benchmark, $m_t = v_t$. Then

$$\bar{x}_t = \frac{\kappa}{\gamma\sigma_\eta^2 - \lambda}(v_t - p_t),$$

and substituting into (8) gives

$$\begin{aligned} dp_t &= \kappa(v_t - p_t)dt + \lambda \frac{\kappa}{\gamma\sigma_\eta^2 - \lambda}(v_t - p_t)dt + \sigma_\eta dZ_t \\ &= -\kappa_{\text{eff}}(p_t - v_t)dt + \sigma_\eta dZ_t, \end{aligned}$$

where

$$\kappa_{\text{eff}} := \kappa \left(1 + \frac{\lambda}{\gamma\sigma_\eta^2 - \lambda} \right) = \kappa \frac{\gamma\sigma_\eta^2}{\gamma\sigma_\eta^2 - \lambda}.$$

Define $y_t := p_t - v_t$. Using $dv_t = \mu_v dt + \sigma_v dW_t$,

$$dy_t = dp_t - dv_t = -\kappa_{\text{eff}}y_t dt - \mu_v dt + \sigma_\eta dZ_t - \sigma_v dW_t,$$

as claimed. If $\gamma\sigma_\eta^2 > \lambda$ then $\kappa_{\text{eff}} > 0$ and y_t is an OU process. When $\mu_v = 0$, y_t has diffusion variance rate $\sigma_\eta^2 + \sigma_v^2$ and mean-reversion rate κ_{eff} , so its stationary variance is

$$\text{Var}(y_\infty) = \frac{\sigma_\eta^2 + \sigma_v^2}{2\kappa_{\text{eff}}}.$$

\square

6 Numerical Examples

Design. We compute summary statistics for the *myopic mean-field consistent dynamics* in Sections II–IV using a particle approximation: simulate N agents with shared common shocks (W, U, Z) and independent idiosyncratic signal noises $\{B_i\}$, with trading governed by the myopic rule (29) and belief updates given by the Kalman filter in Appendix A (implemented in discrete time via Euler/Kalman recursions). We report four baseline scenarios: (i) bull regime ($\mu_v > 0$) with $k = 1$, (ii) bull regime with $k = 3$, (iii) bear regime ($\mu_v < 0$) with $k = 1$, (iv) bear regime with $k = 3$. Each scenario is averaged over M independent random seeds.

Algorithm 2 Particle approximation (one scenario)

- 1: Fix parameters, scenario (μ_v, k) , horizon T , population size N , and seeds $m = 1, \dots, M$.
- 2: **for** $m = 1$ to M **do**
- 3: Simulate one realization of common shocks $(\Delta W_t, \Delta U_t, \Delta Z_t)_{t=0}^{T-1}$.
- 4: Initialize (v_0, p_0) and agent beliefs $(\hat{v}_{i,0}, \Sigma_{i,0})$ for $i = 1, \dots, N$.
- 5: **for** $t = 0$ to $T - 1$ **do**
- 6: For each agent i , draw idiosyncratic signal noise $\Delta B_{i,t}$ and update $(\hat{v}_{i,t}, \Sigma_{i,t})$ via the (perceived) Kalman recursion.
- 7: Compute demands $x_{i,t}$ from the myopic rule with the per-step fixed point \bar{x}_t (Proposition 4.5).
- 8: Update (v_{t+1}, p_{t+1}) using the Euler discretization of (8).
- 9: **end for**
- 10: Record seed-level time series (price, fundamental, returns, mispricing, demand moments).
- 11: **end for**
- 12: Report scenario figures/tables by averaging statistics across seeds (Monte Carlo over the common and idiosyncratic shocks).

Implementation. Simulations and plotting are reproducible from the repository using `code/scripts/build_paper_artifacts.py`, which writes run-level CSVs and aggregated figures into `paper_artifacts/`. Table 1 lists the baseline parameters. The baseline impact/noise parameters satisfy the stability condition in Proposition 4.7 ($\gamma\sigma_\eta^2 > \lambda$). Unless otherwise stated, we use time step $\Delta t = 1$; Table 7 reports a coarse time-step sensitivity check. **Timing.** Within each discrete step $t \rightarrow t + 1$, agents (i) observe their private signal and update $(\hat{v}_{i,t}, \Sigma_{i,t})$, (ii) choose $x_{i,t}$ from the myopic rule and the per-step fixed point, (iii) the price p_{t+1} realizes from the Euler update of (8), and (iv) in the price-augmented robustness variant, agents incorporate p_{t+1} via the implicit observation in Appendix A (updating beliefs for time $t + 1$). Thus, no future price information is used at decision time.

LQG fixed-point verification (continuous-time demo). As a numerical diagnostic for the constructive LQG solver in Section 3.7, we run `code/matlab/mfg_lqg_common_noise_demo.m` with $\Delta t = 10^{-3}$ and $N = 2000$. The Picard fixed point converges in 16 iterations with final relative residual 9.59×10^{-7} . Over the time grid, the reported RMS differences between the particle approximation and the limiting paths are: 8.52×10^{-3} for the mean belief m , 2.09×10^{-3} for the price p , 8.42×10^{-3} for the mean demand \bar{x} , and 7.13×10^{-3} for the disagreement variance benchmark. **Scheme (map form).** Let $S_t = (v_t, p_t, \{(\hat{v}_{i,t}, \Sigma_{i,t})\}_{i=1}^N)$. For fixed shocks (common and idiosyncratic) the algorithm defines a measurable one-step map

$$S_{t+1} = \Psi_{\Delta t, N}(S_t; \text{shocks}), \quad (62)$$

obtained by composing: (a) the Kalman update (Appendix A), (b) the per-step mean-field fixed point (Theorem 4.6), and (c) the Euler updates for (v, p) . Under the contraction condition (53), the fixed-point step is stable and the full map is well-defined (Theorem 3.1).

6.1 Parameter identification and calibration strategy

While full empirical estimation is beyond the scope of this paper, we provide an identification argument showing which observable moments pin down the key structural parameters $(\kappa, \lambda, \sigma_\eta, \sigma_\epsilon, \sigma_v)$ in principle. This clarifies what data would be needed for calibration and establishes the model's testability.

Table 1: Model and numerical parameters.

Parameter	Description	Baseline Value	Units
<i>Model Parameters</i>			
γ	Risk aversion	1.0	—
k	Overconfidence (signal precision scale)	1.0, 3.0	—
μ_v	Fundamental drift (bull/bear)	± 0.02	value/step
σ_v	Fundamental volatility	0.10	value/ $\sqrt{\text{step}}$
σ_c	Common signal component	0.10	value/ $\sqrt{\text{step}}$
σ_ϵ	Idiosyncratic signal noise	0.80	value/ $\sqrt{\text{step}}$
κ	Fundamental anchoring	0.005	1/step
λ	Impact strength	0.20	value/(demand·step)
σ_η	Price/noise-trading volatility	0.50	value/ $\sqrt{\text{step}}$
<i>Numerical Parameters</i>			
N	Number of agents	200	—
T	Horizon (steps)	400	step
M	Random seeds (replications)	50	—
p_0	Initial price	0.0	value
v_0	Initial fundamental	0.0	value

Identification via observable moments. Under the myopic mean-field equilibrium, the following moments are observable (or proxied) from price and volume data:

1. **Return volatility** $\text{std}(r_t)$: In the model, “return” is the price increment $r_t := \Delta p_t$ (value units), not log returns. From (8), the price increment variance is

$$\text{Var}(dp_t) \approx \kappa^2 \text{Var}(v_t - p_t) dt + \lambda^2 \text{Var}(\bar{x}_t) dt + \sigma_\eta^2 dt + \text{cross terms}.$$

In steady state, $\text{std}(r_t) = \text{std}(\Delta p_t)$ depends on σ_η (direct noise trading), λ (impact amplification), and κ (mean reversion strength). The ratio λ/κ can be identified from the relative contribution of demand-driven vs. fundamental-driven price variance.

2. **Mean-reversion speed:** The autocorrelation of price deviations from a moving average of fundamentals (or a proxy like a slow-moving average of prices) identifies κ . Specifically, under (8), the half-life of price deviations is approximately $(\ln 2)/\kappa$, so κ can be estimated from the decay rate of price-f fundamental autocorrelations.
3. **Impact coefficient λ :** The contemporaneous correlation between order flow (aggregate demand proxy) and price changes, normalized by the variance of order flow, identifies λ up to the mean-field scaling. Volume proxies (e.g., signed volume or turnover) can serve as demand proxies.

Scenario	$\mathbb{E}[p - v]$	$\mathbb{E}[\sigma_i(\hat{v}_i)]$	$\mathbb{E}[\sigma_i(x_i)]$	$\mathbb{E}[\Sigma]$
Bull $k = 1$	1.578 ± 0.392	0.206 ± 0.003	0.004 ± 0.000	0.080 ± 0.000
Bull $k = 3$	1.576 ± 0.392	0.264 ± 0.004	0.005 ± 0.000	0.044 ± 0.000
Bear $k = 1$	1.515 ± 0.436	0.206 ± 0.003	0.004 ± 0.000	0.080 ± 0.000
Bear $k = 3$	1.512 ± 0.441	0.264 ± 0.004	0.005 ± 0.000	0.044 ± 0.000
Δ Bull ($k = 3 - 1$)	-0.002 ± 0.005	0.058 ± 0.000	0.001 ± 0.000	-0.036 ± 0.000
Δ Bear ($k = 3 - 1$)	-0.004 ± 0.005	0.058 ± 0.000	0.001 ± 0.000	-0.036 ± 0.000

Table 2: Belief and market moments by scenario (mean \pm 95% CI across random seeds).

Scenario	$\mathbb{E}[p - v]$	$q_{0.95}(p - v)$	$q_{0.99}(p - v)$	$\rho_1(p - v)$	$\rho_1(p - v)$
Bull $k = 1$	1.578 ± 0.392	3.500 ± 0.665	3.937 ± 0.763	0.887 ± 0.050	0.944 ± 0.016
Bull $k = 3$	1.576 ± 0.392	3.492 ± 0.661	3.931 ± 0.764	0.887 ± 0.050	0.944 ± 0.016
Bear $k = 1$	1.515 ± 0.436	3.299 ± 0.850	3.947 ± 0.975	0.869 ± 0.039	0.946 ± 0.015
Bear $k = 3$	1.512 ± 0.441	3.300 ± 0.861	3.949 ± 0.986	0.868 ± 0.039	0.945 ± 0.015
Δ Bull ($k = 3 - 1$)	-0.002 ± 0.005	-0.008 ± 0.021	-0.006 ± 0.023	0.000 ± 0.001	-0.000 ± 0.000
Δ Bear ($k = 3 - 1$)	-0.004 ± 0.005	0.001 ± 0.016	0.002 ± 0.019	-0.001 ± 0.001	-0.000 ± 0.000

Table 3: Mispricing tails and persistence diagnostics by scenario (mean \pm 95% CI across random seeds).

4. **Fundamental volatility σ_v :** The long-run variance of fundamentals (estimated from a slow-moving filter of prices or from fundamental proxies like earnings/dividends) identifies σ_v . Alternatively, σ_v can be identified from the steady-state variance of the Kalman filter innovation process.
5. **Signal noise σ_ϵ :** The cross-sectional dispersion in beliefs (proxied by analyst forecast dispersion or survey-based disagreement) relative to the fundamental variance identifies the signal-to-noise ratio σ_v/σ_ϵ . Given σ_v , this pins down σ_ϵ .

Baseline parameterization. The baseline values in Table 1 are chosen to satisfy the stability condition $\gamma\sigma_\eta^2 > \lambda$ and to generate return volatilities and mean-reversion speeds in a reasonable range for daily/weekly financial data. Specifically:

- $\kappa = 0.005$ implies a half-life of price deviations around 140 steps (roughly consistent with mean-reversion speeds observed in equity markets).
- $\lambda = 0.20$ and $\sigma_\eta = 0.50$ yield $\lambda/\kappa = 40$ and $\gamma\sigma_\eta^2 - \lambda > 0$ (stability), generating price-increment volatilities $\text{std}(\Delta p)$ in the 0.5–1.0 range per step (value units).
- $\sigma_v = 0.10$ and $\sigma_\epsilon = 0.80$ yield a signal-to-noise ratio $\sigma_v/\sigma_\epsilon = 0.125$, consistent with moderate information quality in private signals.

A full calibration would target these moments jointly via method of moments or maximum likelihood on price/volume panel data. The identification argument above shows that the model is in principle testable given appropriate data.

6.2 One-asset moment match vignette

We illustrate how the identification mapping in §6.1 can be operationalized using a single liquid ETF (SPY).

N	$\Delta\mathbb{E}[p - v]$	$\Delta\mathbb{E}[\sigma_i(\hat{v}_i)]$	$\Delta\mathbb{E}[\sigma_i(x_i)]$	$\Delta\mathbb{E}[\Sigma]$
200	0.001 ± 0.001	-0.001 ± 0.001	-0.000 ± 0.000	0.000 ± 0.000
500	0.000 ± 0.001	0.000 ± 0.001	0.000 ± 0.000	0.000 ± 0.000
2000	0.000 ± 0.000	0.000 ± 0.000	0.000 ± 0.000	0.000 ± 0.000

Table 4: Particle convergence check in N (Bull $k = 1$; mean \pm 95% CI across paired seeds; reported as differences relative to the largest N).

λ	$\Delta\mathbb{E}[p - v]$	$\Delta\mathbb{E}[\sigma_i(\hat{v}_i)]$	$\Delta\mathbb{E}[\sigma_i(x_i)]$	$\Delta\mathbb{E}[\Sigma]$
0.10	-0.002 ± 0.002	0.058 ± 0.000	0.001 ± 0.000	-0.036 ± 0.000
0.20	-0.004 ± 0.006	0.058 ± 0.000	0.001 ± 0.000	-0.036 ± 0.000
0.24	-0.007 ± 0.009	0.058 ± 0.000	0.001 ± 0.000	-0.036 ± 0.000

Table 5: Sensitivity of the k -effect to impact strength λ (Bull regime; Δ denotes $k = 3$ minus $k = 1$; mean \pm 95% CI across paired seeds).

Units and mapping. One simulation step corresponds to one trading day; half-life in days maps directly to κ per step. The model (8) uses the *price increment* dp_t (i.e., Δp in value units), not log returns $\Delta \log p$ or simple returns $\Delta p/p$. Because the simulation produces $\text{std}(\Delta p)$ in abstract value units while empirical data report log-return volatility $\sigma_r = \text{std}(\Delta \log P)$, we introduce a scaling constant s such that the empirical target is $\sigma_r \approx s \text{sd}(\Delta p)$. Table 8 calibrates the *effective* composite $s\phi$ (not $\phi = \lambda\sigma_\eta$ directly) to match σ_r ; given a chosen λ , one backs out $\sigma_\eta = (s\phi)/(s\lambda) = \phi/\lambda$ in model units.

From daily adjusted-close data (MacroTrends; 8,306 trading days, 1993–2026), we estimate: (i) an anchoring/mean-reversion rate κ from a half-life diagnostic, and (ii) the unconditional return volatility σ_r as a calibration target.

Auditable estimation procedure. The script `code/scripts/estimate_moment_match.py` implements the following, fully reproducible from the data. (i) **Half-life formula:** Under the OU/AR(1) mapping, the half-life of mean reversion is $h = (\ln 2)/\kappa$, hence $\kappa = (\ln 2)/h$ per trading day. (ii) **Estimating κ from the proxy mispricing series:** We form $y_t := \ln P_t - \ln(\text{MA}_t)$, where MA_t is a slow moving average (200-day, or $\min(200, n/4)$ for shorter series), as a proxy for $(p_t - v_t)$. We fit the AR(1) model $y_t = \rho y_{t-1} + \varepsilon_t$ and obtain the half-life $h = -\ln(0.5)/\ln(\rho)$ days; then $\kappa = (\ln 2)/h$. For SPY we obtain $h \approx 80.8$ days, hence $\kappa \approx 0.0086$ per trading day. (iii) **Mapping σ_r to ϕ :** From (8), the return variance $\text{Var}(dp_t)$ depends on κ , λ , σ_η , and fundamental variance; price-only data primarily identify the *effective impact volatility* $\phi := \lambda\sigma_\eta$ (the product governing demand-driven price noise) rather than λ and σ_η separately. Identifying λ itself requires order-flow proxy data (e.g., signed volume or turnover); in this vignette we treat λ as *externally normalized*. We use the realized daily return volatility $\sigma_r \approx 0.0117$ (annualized ≈ 0.1862) as a calibration target for ϕ , and given an external λ , back out $\sigma_\eta = \phi/\lambda$. Our model baseline uses $\kappa = 0.005$ (half-life ≈ 139 days), so SPY maps to a baseline/high-anchoring regime.

Results. Table 8 reports the moment match and regime classification. The estimates are produced by running `python code/scripts/estimate_moment_match.py -ticker SPY -csv <path>`; outputs are written to `paper_artifacts/moment_match/`. Figure 1 plots the estimated κ against the baseline and stress regions (regime is determined by anchoring strength κ). SPY is

Filter	$\Delta \mathbb{E}[p - v]$	$\Delta \mathbb{E}[\sigma_i(\hat{v}_i)]$	$\Delta \mathbb{E}[\sigma_i(x_i)]$	$\Delta \mathbb{E}[\Sigma]$
Private-only	-0.003 ± 0.006	0.058 ± 0.000	0.001 ± 0.000	-0.036 ± 0.000
Private + price	-0.003 ± 0.006	0.058 ± 0.000	0.001 ± 0.000	-0.036 ± 0.000

Table 6: Robustness to incorporating a noisy price observation in filtering (Bull regime; Δ denotes $k = 3$ minus $k = 1$; mean \pm 95% CI across paired seeds).

Δt	$\Delta \mathbb{E}[p - v]$	$\Delta \mathbb{E}[\sigma_i(\hat{v}_i)]$	$\Delta \mathbb{E}[\sigma_i(x_i)]$	$\Delta q_{0.99}(p - v)$
1.00	-0.008 ± 0.009	0.058 ± 0.000	0.001 ± 0.000	-0.017 ± 0.019
0.50	-0.004 ± 0.005	0.050 ± 0.000	0.001 ± 0.000	-0.005 ± 0.007
0.25	-0.003 ± 0.005	0.042 ± 0.000	0.001 ± 0.000	-0.003 ± 0.011

Table 7: Time-step sensitivity (Bull regime; Δ denotes $k = 3$ minus $k = 1$; mean \pm 95% CI across paired seeds).

in the *baseline* regime with half-life ≈ 81 trading days. The daily return volatility $\sigma_r \approx 1.2\%$ is a calibration target; price-only data identify $\phi = \lambda\sigma_\eta$ up to normalization, not λ and σ_η separately.

Why mispricing does not move with k : architecture bridge. Our model architecture explains why mispricing remains largely unchanged when increasing k across the joint grid (Subsection 6.3.3) and one-at-a-time sweeps (Subsection 6.3.4). Overconfidence k enters only through the Kalman filter (Appendix A): it scales the perceived signal precision $R'_i = \sigma_\epsilon^2/k$, so higher k yields tighter beliefs and more aggressive demand. But the price dynamics (8) have two channels: (a) $\kappa(v_t - p_t)$ pulls the price toward fundamentals (arbitrage/anchoring), and (b) $\lambda\bar{x}_t$ reflects demand impact. Under strong anchoring (high κ), the $\kappa(v_t - p_t)$ term dominates: prices track fundamentals regardless of belief dispersion. Thus k loads mainly onto disagreement and trading intensity (belief dispersion, perceived precision, demand aggressiveness) rather than onto the price level itself. This structural separation— k shifts dispersion and intensity, whereas $(\kappa, \lambda, \sigma_\eta)$ govern mispricing magnitudes—matches what we report in Tables 2–9.

Caveats. The fundamental v_t is unobservable; the moving average is a rough proxy.

6.3 Parameter regimes and stress diagnostics

Preview of findings. Two distinct notions matter in this model: (i) *level amplification*—large mispricing/volatility levels under weak anchoring and/or high noise trading; and (ii) *overconfidence (treatment) effects*—differences in outcomes when increasing perceived signal precision from $k = 1$ to $k = 3$. Our simulations show substantial *level amplification* under stress regimes (Table 14), while the incremental k -effects on average mispricing are modest in both baseline and stress calibrations (Tables 2–3).

6.3.1 Stress regimes: when mispricing *levels* become economically large

Table 14 reports “stress diagnostics” in which anchoring is weakened (κ reduced) and/or noise trading increases (σ_η increased). Weak anchoring and high σ_η generate large mispricing and volatility *levels* (e.g., $\mathbb{E}[|p - v|]$ exceeding 3–9 in stress cases vs. ≈ 1.9 in baseline). **Importantly, these level shifts are primarily driven by (κ, σ_η) : within each stress case, outcomes are nearly unchanged between $k = 1$ and $k = 3$.** This demonstrates that level amplification

Table 8: SPY moment match and regime classification (daily units).

Quantity	Estimate	Baseline	Notes
Anchoring rate κ	0.0086	0.005	$\kappa = (\ln 2)/h$
Half-life h (days)	80.8	139	implied by κ
Return vol σ_r	0.0117	—	calibration target
Effective impact vol $\phi = \lambda\sigma_\eta$ (calibrate)	—	—	identified from σ_r
Regime	baseline	baseline	high anchoring

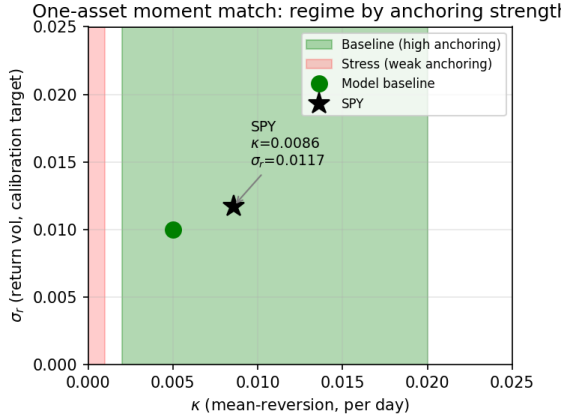


Figure 1: One-asset moment match: estimated κ for SPY vs. baseline and stress regions (regime by anchoring strength). σ_r shown as calibration target.

comes from market microstructure parameters (anchoring strength, noise trading) rather than the overconfidence treatment.

6.3.2 Baseline benchmark: k primarily increases disagreement and trading intensity

We next report the baseline bull/bear scenarios under the benchmark calibration (Table 1). In this parameterization, increasing overconfidence primarily increases cross-sectional disagreement and trading intensity (e.g., $\Delta \mathbb{E}[\sigma_i(\hat{v}_i)] \approx +0.059$ and $\Delta \mathbb{E}[\sigma_i(x_i)] \approx +0.001$), while changes in mean absolute mispricing remain modest ($|\Delta \mathbb{E}[|p - v|]| \approx 0.004$). Mispricing tail and persistence diagnostics (Table 3) are essentially unchanged across k . This baseline serves as a robustness check: it demonstrates that the model does not always amplify mispricing, and that overconfidence's primary channel is through belief dispersion and trading intensity rather than price levels.

6.3.3 Targeted joint-move grid: k -effects on mispricing are robustly small

A natural concern is that one-at-a-time sweeps may miss interaction effects: overconfidence-induced amplification might require *simultaneous* changes in anchoring strength, price impact, and noise trading. To test this directly, we run a targeted $3 \times 3 \times 3$ grid over $(\kappa, \lambda, \sigma_\eta)$ in the bull regime using paired random seeds and compare $k = 3$ against $k = 1$ within each cell.

Table 9 reports cell-by-cell differences in key diagnostics, and Figures 2–3 visualize the resulting treatment effects. We classify a cell as *non-negligible* if (i) the 95% confidence interval for $\Delta_k \mathbb{E}[|p - v|]$ excludes zero and (ii) $|\Delta_k \mathbb{E}[|p - v|]|$ exceeds 5% of the baseline $\mathbb{E}[|p - v|]$ in the same cell.

σ_η	κ	λ	$\Delta \mathbb{E}[p - v]$	$\Delta \mathbb{E}[\sigma_i(\hat{v}_i)]$	$\Delta \mathbb{E}[x_i]$	$\Delta \text{std}(\sum_i x_i)$	$\Delta \text{std}(r)$	Flag
0.25	0.001	0.10	0.000 ± 0.003	0.058 ± 0.001	0.000 ± 0.000	0.008 ± 0.040	-0.000 ± 0.000	
0.25	0.001	0.20	-0.001 ± 0.007	0.058 ± 0.001	0.000 ± 0.000	0.011 ± 0.061	-0.000 ± 0.000	
0.25	0.001	0.50	-0.008 ± 0.014	0.058 ± 0.001	0.000 ± 0.001	0.021 ± 0.066	-0.000 ± 0.000	
0.25	0.005	0.10	-0.002 ± 0.008	0.058 ± 0.001	0.001 ± 0.001	0.038 ± 0.171	-0.000 ± 0.000	
0.25	0.005	0.20	-0.007 ± 0.014	0.058 ± 0.001	0.001 ± 0.002	0.062 ± 0.159	-0.000 ± 0.000	
0.25	0.005	0.50	-0.017 ± 0.008	0.058 ± 0.001	0.002 ± 0.001	0.204 ± 0.139	0.000 ± 0.000	✓
0.25	0.020	0.10	-0.007 ± 0.012	0.058 ± 0.001	0.004 ± 0.005	0.285 ± 0.417	0.000 ± 0.000	
0.25	0.020	0.20	-0.014 ± 0.010	0.058 ± 0.001	0.006 ± 0.003	0.454 ± 0.354	0.000 ± 0.000	
0.25	0.020	0.50	-0.016 ± 0.005	0.058 ± 0.001	0.002 ± 0.002	0.294 ± 0.183	0.001 ± 0.001	✓
0.50	0.001	0.10	0.000 ± 0.001	0.058 ± 0.001	-0.000 ± 0.000	-0.001 ± 0.006	-0.000 ± 0.000	
0.50	0.001	0.20	-0.000 ± 0.003	0.058 ± 0.001	-0.000 ± 0.000	-0.003 ± 0.019	-0.000 ± 0.000	
0.50	0.001	0.50	-0.000 ± 0.004	0.058 ± 0.001	-0.000 ± 0.000	-0.002 ± 0.011	-0.000 ± 0.000	
0.50	0.005	0.10	0.000 ± 0.002	0.058 ± 0.001	0.000 ± 0.000	-0.006 ± 0.034	-0.000 ± 0.000	
0.50	0.005	0.20	-0.001 ± 0.007	0.058 ± 0.001	-0.000 ± 0.001	-0.023 ± 0.085	-0.000 ± 0.000	
0.50	0.005	0.50	-0.002 ± 0.009	0.058 ± 0.001	0.000 ± 0.000	-0.015 ± 0.045	-0.000 ± 0.000	
0.50	0.020	0.10	-0.001 ± 0.004	0.058 ± 0.001	0.000 ± 0.001	-0.021 ± 0.132	-0.000 ± 0.000	
0.50	0.020	0.20	-0.004 ± 0.009	0.058 ± 0.001	-0.000 ± 0.002	-0.024 ± 0.242	-0.000 ± 0.000	
0.50	0.020	0.50	-0.005 ± 0.010	0.058 ± 0.001	0.000 ± 0.001	-0.002 ± 0.122	-0.000 ± 0.000	
1.50	0.001	0.10	-0.000 ± 0.000	0.058 ± 0.001	-0.000 ± 0.000	-0.000 ± 0.000	-0.000 ± 0.000	
1.50	0.001	0.20	-0.000 ± 0.000	0.058 ± 0.001	-0.000 ± 0.000	-0.000 ± 0.000	-0.000 ± 0.000	
1.50	0.001	0.50	-0.000 ± 0.000	0.058 ± 0.001	-0.000 ± 0.000	-0.000 ± 0.001	-0.000 ± 0.000	
1.50	0.005	0.10	0.000 ± 0.000	0.058 ± 0.001	-0.000 ± 0.000	-0.001 ± 0.002	-0.000 ± 0.000	
1.50	0.005	0.20	0.000 ± 0.000	0.058 ± 0.001	-0.000 ± 0.000	-0.001 ± 0.002	-0.000 ± 0.000	
1.50	0.005	0.50	0.000 ± 0.001	0.058 ± 0.001	-0.000 ± 0.000	-0.001 ± 0.003	-0.000 ± 0.000	
1.50	0.020	0.10	-0.000 ± 0.000	0.058 ± 0.001	-0.000 ± 0.000	-0.005 ± 0.011	-0.000 ± 0.000	
1.50	0.020	0.20	-0.000 ± 0.001	0.058 ± 0.001	-0.000 ± 0.000	-0.005 ± 0.011	-0.000 ± 0.000	
1.50	0.020	0.50	-0.000 ± 0.002	0.058 ± 0.001	-0.000 ± 0.000	-0.006 ± 0.013	-0.000 ± 0.000	

Table 9: Joint-grid treatment effects Δ_k across $(\kappa, \lambda, \sigma_\eta)$ (Bull regime; Δ denotes $k = 3$ minus $k = 1$; mean $\pm 95\%$ CI across paired seeds; “Flag” per thresholds in text).

Negative result (robust across the joint grid). Across the full joint grid, $k = 3 - 1$ differences in $\mathbb{E}[|p - v|]$ are statistically indistinguishable from zero and economically small, even in cells where weak anchoring and high noise trading generate large *levels* of mispricing. By contrast, disagreement and trading-intensity proxies move systematically with k . In this architecture, overconfidence primarily loads onto belief dispersion and trading intensity rather than price-level mispricing.

6.3.4 One-at-a-time sweeps: why they rarely generate large k -effects

The joint-grid above (Subsection 6.3.3) establishes that we checked the obvious concern: simultaneous changes in $(\kappa, \lambda, \sigma_\eta)$ do not reveal hidden k -driven mispricing amplification. We now report one-at-a-time sweeps over the key levers highlighted by the model: the impact-to-anchoring ratio (λ/κ), signal-to-noise in private information, anchoring strength κ , and regime drift magnitude $|\mu_v|$.

Economic significance (Flag). The “Flag” column in Tables 10–13 and in the joint grid (Table 9) marks cells where the $k = 3 - 1$ effect is *economically meaningful* by the following criteria. *Mispricing:* we flag if $|\Delta \mathbb{E}[|p - v|]| \geq \max(\theta_{\text{abs}}, \theta_{\text{rel}} \times \text{baseline } \mathbb{E}[|p - v|])$. For the one-at-a-time sweeps we use $\theta_{\text{rel}} = 10\%$ and $\theta_{\text{abs}} = 0.10$; for the joint grid we use $\theta_{\text{rel}} = 5\%$ and $\theta_{\text{abs}} = 0$ so that any cell with a nontrivial relative change in mispricing is flagged; the impaired-arbitrage extension (Table 17) uses $\theta_{\text{rel}} = 5\%$ and $\theta_{\text{abs}} = 0.05$. *Return volatility:* we flag if $|\Delta \text{std}(r)| \geq 20\%$ of the baseline $\text{std}(r)$ in that cell. These thresholds are chosen so that “meaningful” corresponds to a material relative change in mispricing (5–10% of baseline) or a substantive change in return volatility (20%); in our baseline, $\mathbb{E}[|p - v|] \approx 1.9$ (Table 2), so

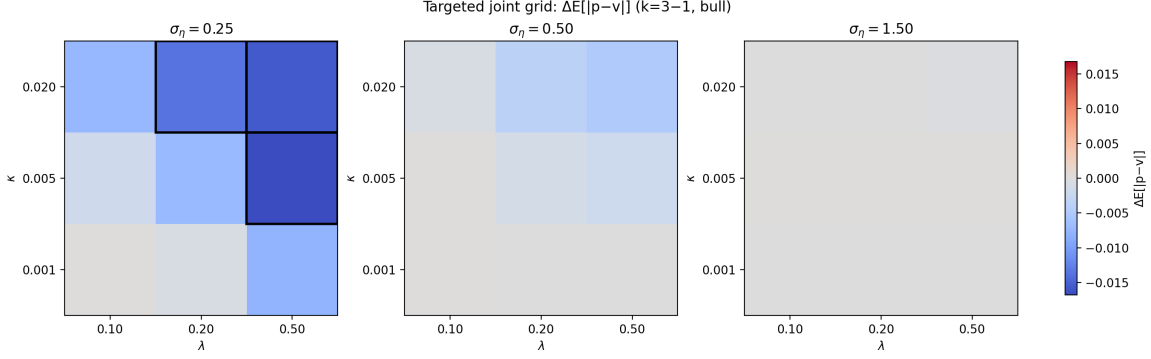


Figure 2: Joint-grid treatment effects $\Delta_k \mathbb{E}[|p - v|]$ across (κ, λ) for three σ_η slices.

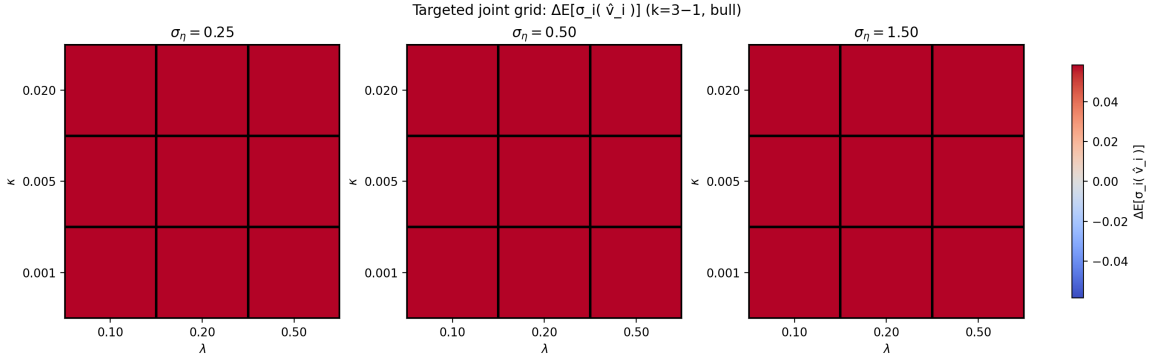


Figure 3: Joint-grid treatment effects on disagreement $\Delta_k \mathbb{E}[\sigma_i(\hat{v}_i)]$ across (κ, λ) for three σ_η slices.

$\theta_{\text{abs}} = 0.10$ is about 5% of baseline. A sensitivity check using $\theta_{\text{rel}} \in \{5\%, 15\%\}$ for mispricing and 15% or 25% for return volatility leaves the set of flagged cells nearly unchanged in our sweeps; the conclusion that k -effects on mispricing are small is robust to these alternatives.

Across one-at-a-time sweeps (Tables 10–13), k -effects on mispricing diagnostics remain small, consistent with the baseline’s strong anchoring channel ($\kappa = 0.005$) suppressing mispricing regardless of other parameters. Even when sweeping impact strength λ up to 0.50 (Table 10), the k -effect on mispricing remains small (often negative) because anchoring remains strong. The sweeps therefore map where outcomes become fragile in *levels* and clarify which parameters would need to be jointly re-estimated in a full calibration exercise targeting economically meaningful mispricing episodes.

6.4 Extensions and Validation Checks

6.4.1 Myopic vs. intertemporal policy

The core qualitative decomposition is robust across equilibrium concepts: the main k -loading remains on disagreement and trading intensity; price-level mispricing is comparatively less sensitive to k under both myopic and intertemporal LQG policies. Comparisons use the same random seeds (paired shocks) and regime parameters; only the policy toggle and k differ. Table 16 and Figures 8–10 report the results. The policy decomposition (Figure 10) confirms the intertemporal hedging term is numerically active. Mispricing is slightly lower under the intertemporal policy than under the myopic rule, and the k -treatment effect remains tiny under both; the modest negative $\Delta \mathbb{E}[|p - v|]$ when increasing k is consistent with stronger perceived precision inducing

λ (impact)	λ/κ	$\Delta E[p - v]$	$\Delta q_{0.95}(p - v)$	$\Delta q_{0.99}(p - v)$	$\Delta \text{std}(r)$	$\Delta \rho_1(r)$	Flag
0.10	20.0	-0.002 ± 0.002	-0.007 ± 0.005	-0.005 ± 0.005	-0.000 ± 0.000	-0.000 ± 0.000	
0.20	40.0	-0.005 ± 0.007	-0.027 ± 0.022	-0.020 ± 0.017	-0.000 ± 0.000	-0.000 ± 0.000	
0.30	60.0	-0.004 ± 0.006	-0.022 ± 0.016	-0.016 ± 0.011	-0.000 ± 0.000	-0.000 ± 0.000	
0.40	80.0	-0.005 ± 0.007	-0.030 ± 0.027	-0.021 ± 0.018	-0.000 ± 0.000	-0.000 ± 0.000	
0.50	100.0	-0.006 ± 0.009	-0.031 ± 0.029	-0.027 ± 0.020	-0.000 ± 0.000	-0.000 ± 0.001	
0.75	150.0	-0.008 ± 0.011	-0.036 ± 0.024	-0.059 ± 0.052	-0.000 ± 0.000	-0.000 ± 0.001	
1.00	200.0	-0.010 ± 0.011	-0.044 ± 0.035	-0.050 ± 0.032	0.000 ± 0.000	-0.001 ± 0.001	

Table 10: Impact-to-anchoring sweep (Bull regime). Δ denotes $k = 3$ minus $k = 1$; “Flag” marks economically meaningful regions (see text for thresholds).

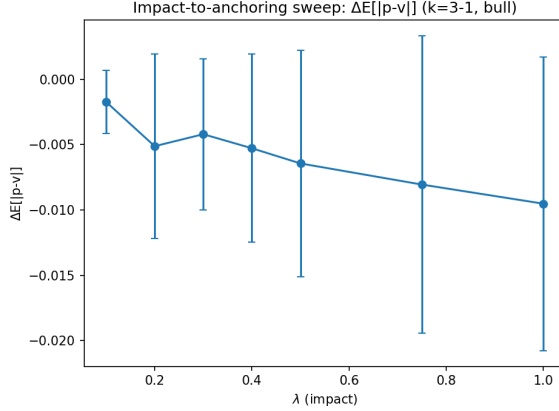


Figure 4: Effect of λ (impact) on $\Delta E[|p - v|]$ (Bull regime; Δ denotes $k = 3$ minus $k = 1$).

faster corrective trading against mispricing under strong anchoring, so price levels do not blow out—what changes with k is dispersion and trading intensity rather than the level of mispricing.

6.4.2 Extension: when k can move mispricing

In the baseline anchored-impact microstructure (relevant for SPY-like regimes), k does not materially move mispricing. When arbitrage pressure is impaired—e.g., via state-dependent anchoring $\kappa(t) = \kappa_0 \exp(-\alpha|p - v|)$ so that κ weakens under large mispricing— k can in principle transmit into price-level mispricing. Table 17 and Figure 11 report the sensitivity to α . In the parameter range shown ($\alpha \in [0, 0.2]$), $\Delta E[|p - v|]$ ($k = 3-1$) remains small (around -0.004 to -0.005); even under modest state-dependence, k -effects on mispricing stay small. Larger arbitrage impairment (e.g., higher α , lower baseline κ_0 , or higher σ_η) would be required for k to materially amplify mispricing. The negative result is not built into linearity; it is regime-specific: in the baseline (strong anchoring), k loads onto disagreement/intensity; in sufficiently impaired-arbitrage regimes, k can amplify mispricing.

6.4.3 Empirical stylized fact: volume and uncertainty/intensity proxy co-movement

We document a stylized fact consistent with the model’s disagreement/intensity channel: volume and an uncertainty/intensity proxy (realized volatility) co-move positively. We cannot directly measure belief dispersion without survey/analyst microdata; we use uncertainty proxies as a reduced-form correlate. This is a well-known generic relationship; we pitch it as external-face validity / sanity check for the model’s intensity channel, not as an identification of “disagreement.” Analyst forecast dispersion, options-implied disagreement, or survey-based disagreement

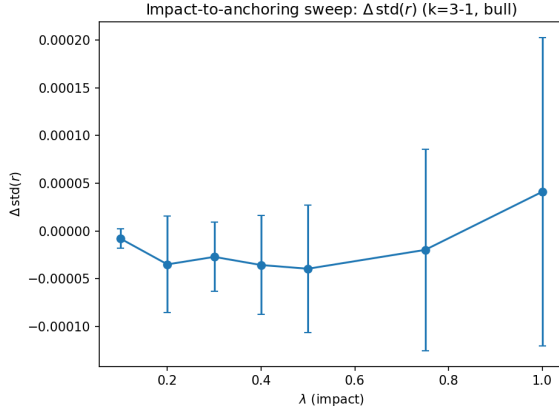


Figure 5: Effect of λ (impact) on $\Delta \text{std}(r)$ (Bull regime; Δ denotes $k = 3$ minus $k = 1$).

σ_ϵ	σ_v/σ_ϵ	$\Delta \mathbb{E}[p - v]$	$\Delta q_{0.95}(p - v)$	$\Delta q_{0.99}(p - v)$	$\Delta \text{std}(r)$	$\Delta \rho_1(r)$	$\Delta \mathbb{E}[\sigma_i(\hat{v}_i)]$	$\Delta \mathbb{E}[\sigma_i(x_i)]$	Flag
0.40	0.250	-0.004 ± 0.008	-0.010 ± 0.015	-0.010 ± 0.011	0.000 ± 0.000	-0.000 ± 0.000	0.037 ± 0.000	0.001 ± 0.000	
0.50	0.200	-0.006 ± 0.010	-0.012 ± 0.013	-0.012 ± 0.015	0.000 ± 0.000	-0.000 ± 0.000	0.044 ± 0.000	0.001 ± 0.000	
0.60	0.167	-0.007 ± 0.012	-0.013 ± 0.014	-0.010 ± 0.019	0.000 ± 0.000	-0.000 ± 0.000	0.049 ± 0.000	0.001 ± 0.000	
0.80	0.125	-0.008 ± 0.016	-0.012 ± 0.019	-0.006 ± 0.028	0.000 ± 0.000	-0.000 ± 0.000	0.059 ± 0.001	0.001 ± 0.000	
1.00	0.100	-0.010 ± 0.020	-0.004 ± 0.025	-0.004 ± 0.034	0.000 ± 0.000	-0.000 ± 0.000	0.067 ± 0.001	0.001 ± 0.000	
1.20	0.083	-0.011 ± 0.024	-0.001 ± 0.028	-0.001 ± 0.040	0.000 ± 0.000	-0.000 ± 0.000	0.075 ± 0.001	0.001 ± 0.000	
2.00	0.050	-0.015 ± 0.038	-0.000 ± 0.041	0.009 ± 0.050	0.000 ± 0.000	0.000 ± 0.000	0.101 ± 0.001	0.002 ± 0.000	

Table 11: Signal-to-noise sweep (Bull regime): varying σ_ϵ while holding σ_v fixed. “Flag” marks economically meaningful regions (see text).

are natural next steps for tighter empirical tests. Stress episodes are defined mechanically as the top decile of realized volatility (no cherry-picking).

Figure 12 plots the rolling correlation; Table 18 reports correlations in stress vs. non-stress with Newey–West t -statistics. Our model provides a mechanism: overconfidence increases disagreement and trading intensity; when both are high, volume and belief dispersion move together.

Baseline results (benchmark). Figure 13 reports the mean price path across baseline scenarios. Figure 14 reports mean absolute mispricing $\mathbb{E}[|p_t - v_t|]$ (computed from the simulated fundamental), and Figure 15 reports a rolling volatility proxy based on realized returns. Table 2 complements the plots with seed-averaged moments and treatment effects ($k = 3$ vs. $k = 1$). **In this baseline parameterization, the k -effect on mispricing is weak ($|\Delta \mathbb{E}[|p-v|]| \approx 0.004$), and mispricing tail/persistence diagnostics (Table 3) are essentially unchanged across k .** Proposition 4.4 explains this analytically: the mean-field closure depends only on the mean belief $m_t - p_t$, so mispricing is driven by microstructure ($\kappa, \lambda, \sigma_\eta$) and the mean-belief error $e_t = m_t - v_t$; under the filter structure, k raises disagreement (strictly in k) and trading intensity while affecting the mean belief only weakly, hence small price effects. Increasing overconfidence primarily increases cross-sectional disagreement and trading intensity (e.g., $\Delta \mathbb{E}[\sigma_i(\hat{v}_i)] \approx +0.059$ and lower perceived $\mathbb{E}[\bar{\Sigma}]$), consistent with that mechanism. The qualitative asymmetry remains visible in paths: bull regimes exhibit more persistent overvaluation episodes, while bear regimes exhibit noisier oscillations around fundamentals.

Discussion. The particle simulations are intended as computational evidence for the feedback mechanism highlighted by the model: misperceived signal precision affects belief dispersion and demand, which in turn impacts prices through (8). A full numerical fixed-point verification for the common-noise mean-field limit (e.g., via conditional-law SPDE solvers) is left for future work. As a robustness check for the informational simplification (filtering on ξ_i only), the artifact script also produces a “price-augmented” filtering variant aligned with the Euler price update: it

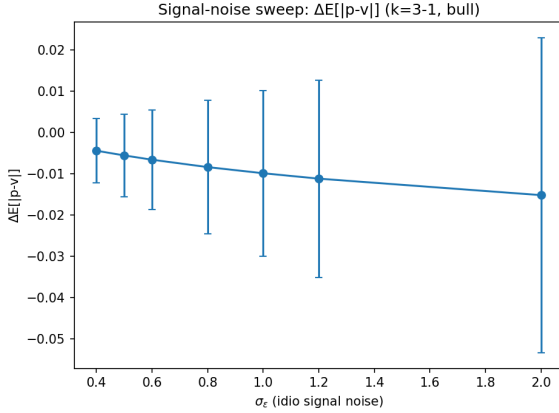


Figure 6: Effect of σ_ϵ on $\Delta\mathbb{E}[|p - v|]$ (Bull regime; Δ denotes $k = 3$ minus $k = 1$).

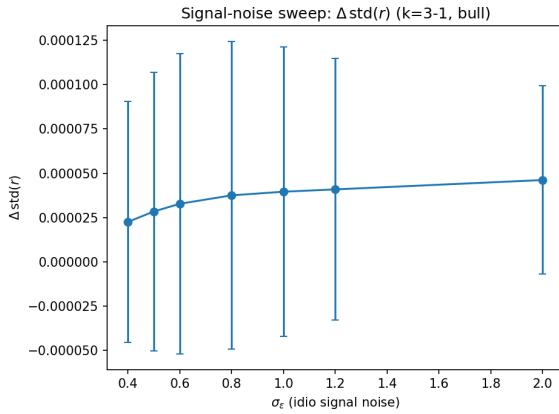


Figure 7: Effect of σ_ϵ on $\Delta \text{std}(r)$ (Bull regime; Δ denotes $k = 3$ minus $k = 1$).

uses the realized increment $p_{t+1} - p_t$ to form an implicit noisy observation of v_t (Appendix A). The qualitative k -effects on perceived uncertainty and disagreement remain similar in that check (Table 6).

7 Conclusion

This paper formulates a mean-field game framework for modeling financial markets with heterogeneous overconfident investors. The model couples Bayesian belief updating (with misperceived signal precision) to endogenous price formation through a stochastic anchored-impact price equation. We derive a checkable CARAbest response under Gaussian price increments and obtain a simple mean-field closure linking mean demand to mean belief.

The simulations demonstrate a clean *mechanism separation*: (i) *mispicing levels* are governed primarily by the microstructure regime $(\kappa, \lambda, \sigma_\eta)$ —weak anchoring and high noise trading generate large mispricing and volatility levels; and (ii) *overconfidence* (k) robustly loads onto disagreement and trading intensity, but does not materially move price-level mispricing across a broad joint grid (Subsection 6.3.3), even when mispricing levels become large. This structural separation— k shifts belief dispersion and intensity, whereas $(\kappa, \lambda, \sigma_\eta)$ govern mispricing magnitudes—is the main empirical takeaway. The identification argument (Section 6.1) makes the model empirically testable, clarifying which observable moments pin down the structural

κ	λ/κ	$\Delta \mathbb{E}[p - v]$	$\Delta q_{0.95}(p - v)$	$\Delta q_{0.99}(p - v)$	$\Delta \text{std}(r)$	$\Delta \rho_1(r)$	Flag
0.001	200.0	0.000 ± 0.004	-0.001 ± 0.009	0.001 ± 0.009	0.000 ± 0.000	0.000 ± 0.000	
0.002	100.0	0.001 ± 0.006	0.005 ± 0.012	0.002 ± 0.014	0.000 ± 0.000	0.000 ± 0.000	
0.003	66.7	0.001 ± 0.008	-0.000 ± 0.014	0.001 ± 0.016	0.000 ± 0.000	0.000 ± 0.000	
0.005	40.0	0.001 ± 0.009	0.005 ± 0.012	0.007 ± 0.015	0.000 ± 0.000	0.000 ± 0.000	
0.010	20.0	-0.000 ± 0.009	-0.010 ± 0.026	-0.006 ± 0.033	0.000 ± 0.000	0.001 ± 0.001	
0.020	10.0	0.000 ± 0.007	-0.008 ± 0.022	-0.006 ± 0.037	0.000 ± 0.000	0.000 ± 0.001	

Table 12: Anchoring sweep (Bull regime): varying κ at fixed (λ, σ_η) . “Flag” marks economically meaningful regions (see text).

Regime	μ_v	$\Delta \mathbb{E}[p - v]$	$\Delta q_{0.95}(p - v)$	$\Delta q_{0.99}(p - v)$	$\Delta \text{std}(r)$	$\Delta \rho_1(r)$	Flag
Bull	0.010	-0.004 ± 0.004	-0.005 ± 0.031	0.006 ± 0.011	0.000 ± 0.000	-0.000 ± 0.000	
Bull	0.020	-0.005 ± 0.004	-0.018 ± 0.021	-0.004 ± 0.018	0.000 ± 0.000	-0.000 ± 0.000	
Bull	0.030	-0.005 ± 0.004	-0.012 ± 0.029	-0.009 ± 0.026	0.000 ± 0.000	-0.000 ± 0.000	
Bull	0.050	-0.005 ± 0.006	-0.006 ± 0.025	-0.009 ± 0.026	0.000 ± 0.000	-0.000 ± 0.000	
Bear	-0.010	-0.005 ± 0.004	0.000 ± 0.021	-0.017 ± 0.008	0.000 ± 0.000	-0.000 ± 0.000	
Bear	-0.020	-0.006 ± 0.004	-0.004 ± 0.017	-0.007 ± 0.019	0.000 ± 0.000	-0.000 ± 0.000	
Bear	-0.030	-0.006 ± 0.004	-0.017 ± 0.005	-0.011 ± 0.016	0.000 ± 0.000	-0.000 ± 0.000	
Bear	-0.050	-0.007 ± 0.005	-0.014 ± 0.011	-0.008 ± 0.016	0.000 ± 0.000	-0.000 ± 0.000	

Table 13: Regime-strength sweep: varying $|\mu_v|$ in bull/bear regimes. “Flag” marks economically meaningful regions (see text).

parameters.

Several limitations and open questions remain. First, the dynamic policy we implement is the myopic CARAbest response under conditionally Gaussian price increments; extending the analysis to fully intertemporal portfolio choice with constraints is of interest. Second, while Sub-section 6.1 provides an identification argument showing which moments pin down $(\kappa, \lambda, \sigma_v, \sigma_\epsilon, \sigma_\eta)$ in principle, a full empirical calibration targeting these moments from price and volume data would strengthen the quantitative predictions. Third, the single-population framework abstracts from strategic and institutional heterogeneity; multi-population extensions (e.g., retail vs. institutional) could produce richer belief distributions and feedback. Finally, while Section III establishes well-posedness and uniqueness of the myopic mean-field fixed point under $\gamma\sigma_\eta^2 > \lambda$ (Theorem 3.2), a complete verification of existence/uniqueness conditions for the full intertemporal optimal-control MFG equilibrium (with endogenous filtering on prices) would strengthen the theoretical foundation.

A Kalman–Bucy Filter With Misperceived Signal Precision

This appendix summarizes the Kalman–Bucy filter used for belief updating in Section II.

A.1 State and Observation Equations

The (unobserved) fundamental evolves as a linear diffusion

$$dv_t = \mu_v dt + \sigma_v dW_t, \quad (63)$$

and investor i observes a private signal

$$d\xi_{i,t} = v_t dt + \sigma_c dU_t + \sigma_\epsilon dB_{i,t}, \quad (64)$$

where W , U , and B_i are independent Brownian motions and U is common across investors.

Scenario	κ	σ_η	$\mathbb{E}[p - v]$		$q_{0.95}(p - v)$		std(r)	
			$k = 1$	$k = 3$	$k = 1$	$k = 3$	$k = 1$	$k = 3$
Baseline	0.005	0.50	1.509 ± 0.288	1.497 ± 0.284	3.769 ± 0.818	3.751 ± 0.827	0.505 ± 0.008	0.505 ± 0.008
Weak anchoring	0.001	0.50	2.260 ± 0.763	2.254 ± 0.760	5.011 ± 1.591	5.002 ± 1.583	0.502 ± 0.008	0.502 ± 0.008
High noise	0.005	1.00	3.466 ± 0.738	3.465 ± 0.737	8.335 ± 1.398	8.333 ± 1.398	1.004 ± 0.016	1.004 ± 0.016
Weak+high	0.001	1.00	3.958 ± 0.966	3.958 ± 0.966	9.019 ± 1.617	9.018 ± 1.617	1.002 ± 0.016	1.002 ± 0.016
Low noise	0.005	0.25	0.618 ± 0.081	0.597 ± 0.075	1.500 ± 0.303	1.473 ± 0.291	0.256 ± 0.005	0.256 ± 0.004
Mid-high noise	0.005	0.75	2.680 ± 0.669	2.677 ± 0.668	6.402 ± 1.328	6.399 ± 1.327	0.753 ± 0.012	0.753 ± 0.012
Very high noise	0.005	1.50	5.012 ± 0.810	5.012 ± 0.810	12.125 ± 1.558	12.125 ± 1.558	1.506 ± 0.024	1.506 ± 0.024
Extreme noise	0.005	2.00	6.587 ± 0.900	6.587 ± 0.900	16.105 ± 1.775	16.105 ± 1.775	2.007 ± 0.031	2.007 ± 0.031
Very weak anchoring	0.001	0.50	2.479 ± 0.885	2.476 ± 0.884	5.400 ± 1.767	5.393 ± 1.764	0.501 ± 0.008	0.501 ± 0.008

Table 14: Stress diagnostics: weakening anchoring (κ) and/or increasing noise trading (σ_η) can generate large mispricing and volatility *levels*. Within each stress case, outcomes are nearly unchanged between $k = 1$ and $k = 3$, indicating that level amplification is primarily driven by (κ, σ_η) rather than the overconfidence treatment.

Case	$\mathbb{E}[p - v]$	$q_{0.95}(p - v)$	$q_{0.99}(p - v)$	std(r)	std _{xs} (k_i)
Fixed k=2.0	2.121 ± 0.819	4.356 ± 1.134	4.987 ± 1.203	0.488 ± 0.020	0.000 ± 0.000
Uniform[1,3] (mean 2)	1.787 ± 0.410	4.118 ± 0.668	4.643 ± 0.796	0.492 ± 0.029	0.558 ± 0.031
Normal(2,0.5) clipped[1,3]	1.787 ± 0.410	4.118 ± 0.668	4.642 ± 0.797	0.492 ± 0.029	0.471 ± 0.026

Table 15: Heterogeneous k at fixed mean $\mathbb{E}[k] = 2$: comparing dispersion in confidence under the same market regime. Column std_{xs}(k_i) is the cross-sectional standard deviation of k_i across agents, time-averaged.

A.2 Filter and Riccati Equation

Let $(\hat{v}_{i,t}, \Sigma_{i,t})$ denote investor i 's Kalman–Bucy belief state computed under the *perceived* measurement-noise variance $R'_i(k_i)$ below. When $k_i = 1$, $\hat{v}_{i,t}$ coincides with the true conditional mean $\mathbb{E}[v_t | \mathcal{F}_t^i]$ and $\Sigma_{i,t}$ with the true conditional variance; when $k_i \neq 1$ they are best interpreted as *subjective* filter states (equivalently, $\hat{v}_{i,t} = \mathbb{E}^{(k_i)}[v_t | \mathcal{F}_t^i]$ under the investor's misspecified noise model).

A.2.1 Belief-mean SDE and diffusion decomposition

The belief state is $(\hat{v}_{i,t}, \Sigma_{i,t})$. Only $\hat{v}_{i,t}$ is stochastic; $\Sigma_{i,t}$ follows a scalar Riccati ODE. Starting from the Kalman–Bucy form

$$\begin{aligned} d\hat{v}_{i,t} &= \mu_v dt + K_{i,t}(d\xi_{i,t} - \hat{v}_{i,t} dt), \\ K_{i,t} &= \frac{\Sigma_{i,t}}{R'_i}, \quad R'_i = \sigma_c^2 + \frac{\sigma_\epsilon^2}{k_i}. \end{aligned} \tag{65}$$

and using the signal SDE $d\xi_{i,t} = v_t dt + \sigma_c dU_t + \sigma_\epsilon dB_{i,t}$, we obtain the explicit diffusion decomposition

$$d\hat{v}_{i,t} = (\mu_v + K_{i,t}(v_t - \hat{v}_{i,t})) dt + K_{i,t}\sigma_c dU_t + K_{i,t}\sigma_\epsilon dB_{i,t}. \tag{66}$$

Thus the belief-mean diffusion has (i) a *common* component $K_{i,t}\sigma_c dU_t$ and (ii) an *idiosyncratic* component $K_{i,t}\sigma_\epsilon dB_{i,t}$. The perceived posterior variance satisfies the Riccati ODE

$$\dot{\Sigma}_{i,t} = \sigma_v^2 - \frac{\Sigma_{i,t}^2}{R'_i}, \tag{67}$$

and carries no diffusion term.

Here R'_i is the *perceived* measurement-noise variance. Overconfidence corresponds to $k_i > 1$, i.e., investors treat their signal as more precise than it truly is. The common component $\sigma_c dU_t$ prevents the law-of-large-numbers collapse of aggregate signal noise in the continuum limit and is the source of common-noise randomness in Section III.

Policy	k	$\mathbb{E}[p - v]$	$q_{0.95}(p - v)$	$\text{std}(r)$
Myopic	1	1.669 ± 0.449	3.799 ± 0.933	0.498 ± 0.021
Myopic	3	1.666 ± 0.444	3.792 ± 0.920	0.498 ± 0.021
Intertemporal	1	1.483 ± 0.342	3.447 ± 0.719	0.499 ± 0.022
Intertemporal	3	1.478 ± 0.333	3.438 ± 0.712	0.499 ± 0.022
Δ Myopic ($k = 3 - 1$)	—	-0.003 ± 0.010	-0.007 ± 0.018	-0.000 ± 0.000
Δ Intertemporal ($k = 3 - 1$)	—	-0.005 ± 0.011	-0.009 ± 0.014	-0.000 ± 0.000

Table 16: Myopic vs. intertemporal policy: $\mathbb{E}[|p - v|]$, $q_{0.95}(|p - v|)$, and $\text{std}(r)$ by policy and k .

α	$\mathbb{E}[p - v] (k = 1)$	$\Delta \mathbb{E}[p - v]$	$\Delta q_{0.5}$	$\Delta q_{0.95}$	Flag
0.00	1.417	-0.001 ± 0.011	0.003	-0.003	✓
0.05	1.431	-0.001 ± 0.011	0.001	-0.003	✓
0.10	1.443	-0.001 ± 0.012	0.004	-0.003	✓
0.20	1.463	-0.001 ± 0.012	0.002	-0.003	✓

Table 17: Impaired-arbitrage extension: $\Delta \mathbb{E}[|p - v|] (k = 3 - 1)$ vs. α (kappa decay rate). “Flag” per thresholds in text.

The scalar Riccati equation admits an explicit solution and converges exponentially to its steady state:

Lemma A.1 (Riccati convergence to steady state). *Fix $R'_i > 0$ and $\sigma_v > 0$ and let Σ_t solve (67) with $\Sigma_0 \geq 0$. Then $\Sigma_t \rightarrow \Sigma^* := \sigma_v \sqrt{R'_i}$ as $t \rightarrow \infty$ and there exist constants $C, c > 0$ (depending on Σ_0, σ_v, R'_i) such that*

$$|\Sigma_t - \Sigma^*| \leq C e^{-ct}, \quad c = \frac{2\sigma_v}{\sqrt{R'_i}}. \quad (68)$$

Consequently, the gain $K_t = \Sigma_t / R'_i$ converges exponentially to $K^* = \sigma_v / \sqrt{R'_i}$.

Proof. Fix $R'_i > 0$ and $\sigma_v > 0$ and consider the scalar Riccati ODE (67):

$$\frac{d\Sigma_t}{dt} = \sigma_v^2 - \frac{\Sigma_t^2}{R'_i}.$$

Let $\Sigma^* := \sigma_v \sqrt{R'_i}$ (the positive equilibrium). Separating variables,

$$\int_{\Sigma_0}^{\Sigma_t} \frac{ds}{\sigma_v^2 - s^2/R'_i} = t.$$

Write $a := \sigma_v / \sqrt{R'_i}$ so that $\sigma_v^2 - s^2/R'_i = \sigma_v^2(1 - (s/\Sigma^*)^2)$ and set $u := s/\Sigma^*$. Then

$$\begin{aligned} \int_{\Sigma_0}^{\Sigma_t} \frac{ds}{\sigma_v^2 - s^2/R'_i} &= \frac{\sqrt{R'_i}}{\sigma_v} \int_{\Sigma_0/\Sigma^*}^{\Sigma_t/\Sigma^*} \frac{du}{1 - u^2} \\ &= \frac{\sqrt{R'_i}}{\sigma_v} (\operatorname{artanh}(u)) \Big|_{\Sigma_0/\Sigma^*}^{\Sigma_t/\Sigma^*}. \end{aligned}$$

Hence

$$\operatorname{artanh}\left(\frac{\Sigma_t}{\Sigma^*}\right) = \operatorname{artanh}\left(\frac{\Sigma_0}{\Sigma^*}\right) + \frac{\sigma_v}{\sqrt{R'_i}} t.$$

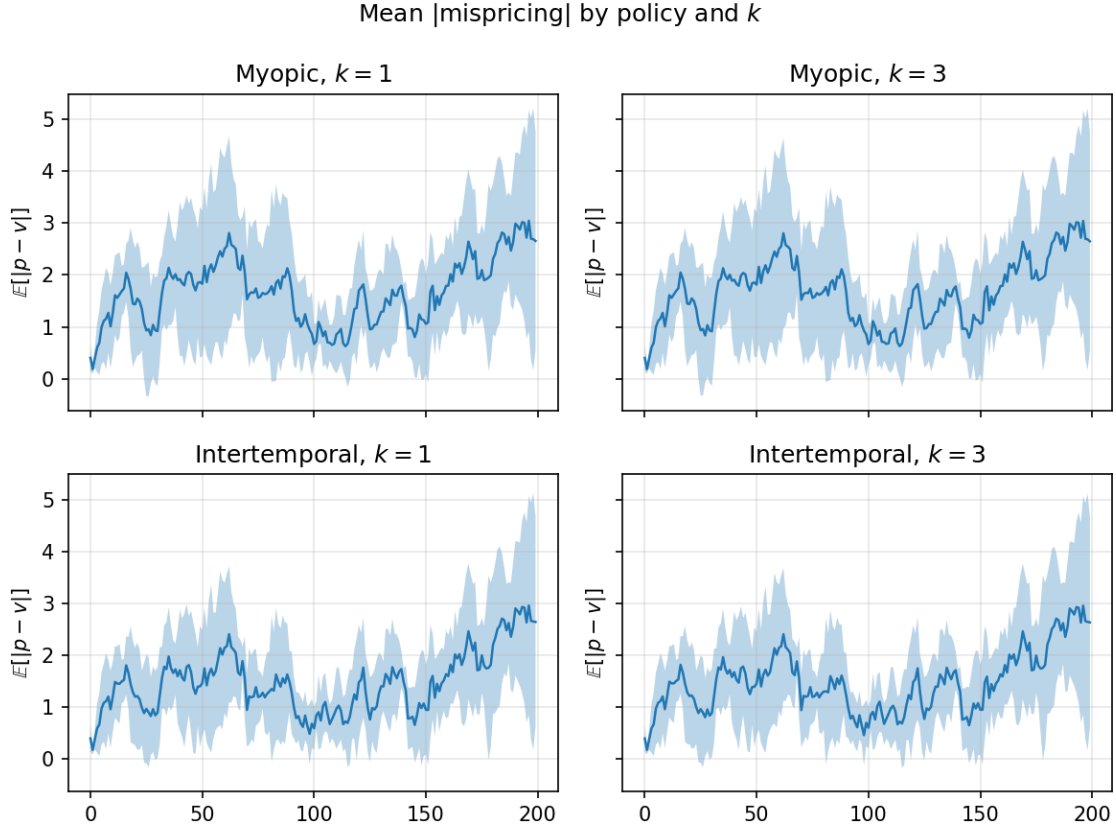


Figure 8: Mean $|p - v|$ by policy (myopic/intertemporal) and k (2×2 grid; 95% CI bands).

Exponentiating via the identity $\tanh(x) = \frac{1-e^{-2x}}{1+e^{-2x}}$ yields the explicit solution

$$\Sigma_t = \Sigma^* \tanh\left(\operatorname{artanh}\left(\frac{\Sigma_0}{\Sigma^*}\right) + \frac{\sigma_v}{\sqrt{R'_i}} t\right) = \Sigma^* \frac{1 - \rho e^{-2at}}{1 + \rho e^{-2at}},$$

where $\rho := \frac{\Sigma^* - \Sigma_0}{\Sigma^* + \Sigma_0}$ and $a := \frac{\sigma_v}{\sqrt{R'_i}}$. (For $\Sigma_0 > \Sigma^*$, the same expression still holds with $\rho < 0$ and is equivalent to a coth representation.) In all cases with $\Sigma_0 \geq 0$, $\Sigma_t \geq 0$ for all t and $\Sigma_t \rightarrow \Sigma^*$ as $t \rightarrow \infty$ since $e^{-2at} \rightarrow 0$.

Moreover,

$$\Sigma_t - \Sigma^* = \Sigma^* \left(\frac{1 - \rho e^{-2at}}{1 + \rho e^{-2at}} - 1 \right) = -\frac{2\Sigma^* \rho e^{-2at}}{1 + \rho e^{-2at}},$$

so

$$|\Sigma_t - \Sigma^*| \leq 2\Sigma^* |\rho| e^{-2at}.$$

Thus the convergence is exponential with rate constant $c = 2a = 2\sigma_v/\sqrt{R'_i}$ and prefactor $C := 2\Sigma^* |\rho|$ (depending on Σ_0, σ_v, R'_i), proving the claimed bound. Since $K_t = \Sigma_t/R'_i$, it follows that $K_t \rightarrow K^* = \Sigma^*/R'_i = \sigma_v/\sqrt{R'_i}$ at the same exponential rate. \square

A.3 Steady State

In steady state, (67) gives

$$\Sigma_i^* = \sigma_v \sqrt{R'_i} = \sigma_v \sqrt{\sigma_c^2 + \frac{\sigma_\epsilon^2}{k_i}}, \quad (69)$$

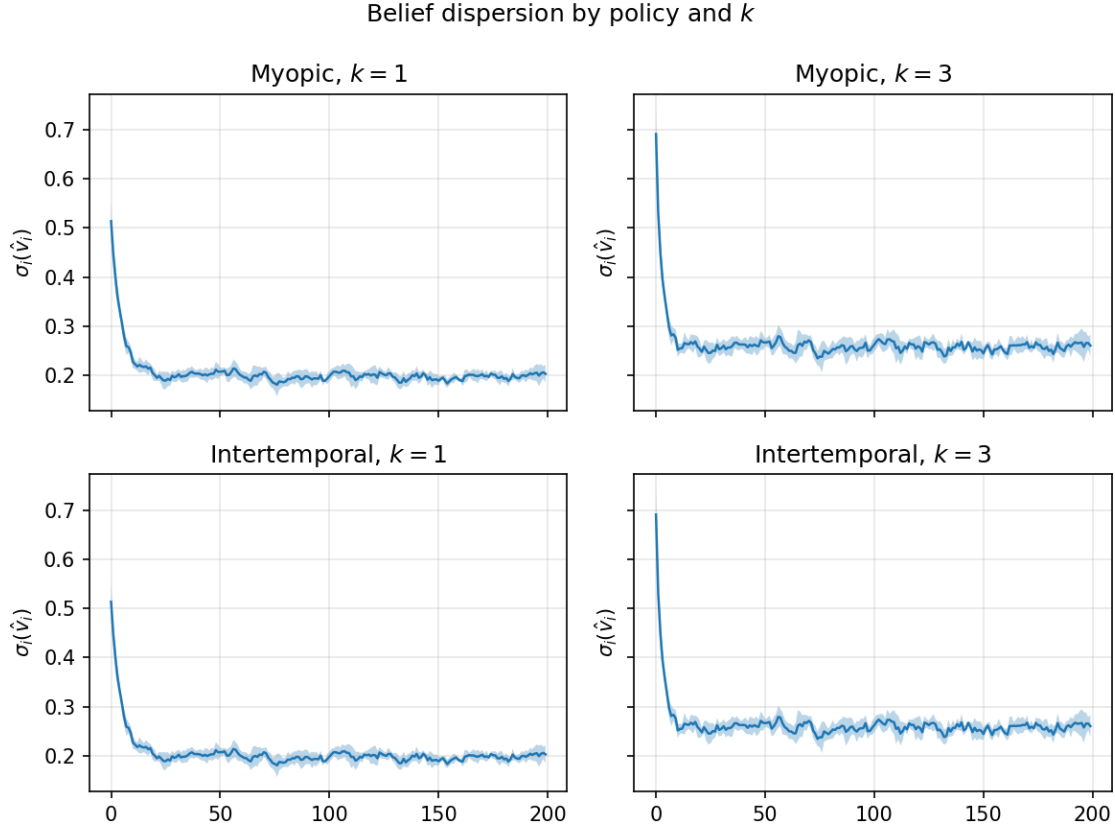


Figure 9: Belief dispersion $\sigma_i(\hat{v}_i)$ by policy and k .

and the corresponding steady-state gain is $K_i^* = \Sigma_i^*/R'_i = \sigma_v/\sqrt{R'_i}$. Thus larger k increases the Kalman gain and reduces perceived posterior variance, generating more aggressive belief updating and, through the trading rule, larger demand responses to perceived mispricing.

A.4 Discrete-Time Recursion Used in Simulations

Section VI implements a discrete-time Kalman recursion (Euler discretization of (65)). With time step $\Delta t = 1$, the simulated fundamental evolves as

$$v_{t+1} = v_t + \mu_v + \sigma_v \varepsilon_{t+1}, \quad \varepsilon_{t+1} \sim \mathcal{N}(0, 1),$$

and investor i observes

$$y_{i,t} = v_t + \sigma_c \varepsilon_t^c + \sigma_\epsilon \varepsilon_{i,t}^i, \quad \varepsilon_t^c, \varepsilon_{i,t}^i \sim \mathcal{N}(0, 1),$$

where ε_t^c is common across investors and $\varepsilon_{i,t}^i$ is idiosyncratic. Overconfidence scales only the idiosyncratic component, so the perceived measurement variance is $R'_i = \sigma_c^2 + \sigma_\epsilon^2/k_i$. Let $(\hat{v}_{i,t}, \Sigma_{i,t})$ denote the posterior mean/variance after processing $y_{i,t}$. The discrete-time Kalman recursion

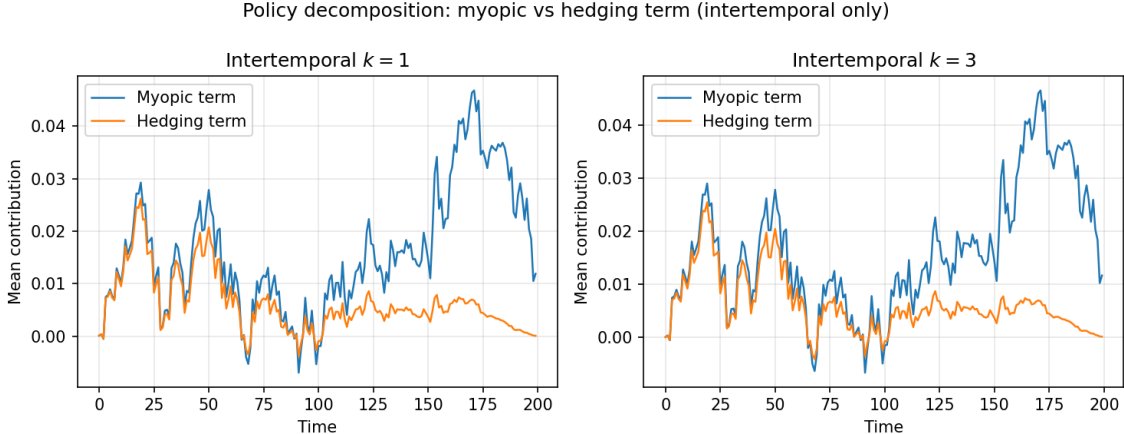


Figure 10: Policy decomposition: myopic vs. hedging term contribution (intertemporal runs).

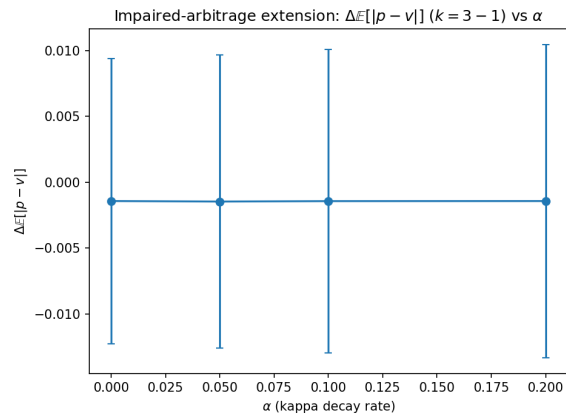


Figure 11: Impaired-arbitrage extension: $\Delta\mathbb{E}[|p - v|]$ ($k = 3 - 1$) vs. α .

(with time step Δt) is:

$$\begin{aligned}\Sigma_{i,t}^- &= \Sigma_{i,t-1} + \sigma_v^2 \Delta t, \\ K_{i,t} &= \frac{\Sigma_{i,t}^-}{\Sigma_{i,t}^- + R'_i}, \\ \hat{v}_{i,t} &= \hat{v}_{i,t-1} + \mu_v \Delta t + K_{i,t} (y_{i,t} - (\hat{v}_{i,t-1} + \mu_v \Delta t)), \\ \Sigma_{i,t} &= (1 - K_{i,t}) \Sigma_{i,t}^-.\end{aligned}$$

Given $\bar{x}_t = \frac{1}{N} \sum_i x_{i,t}$, the discrete-time price update (Euler form of (8)) used in the code is

$$\begin{aligned}p_{t+1} &= p_t + \kappa(v_t - p_t) \Delta t + \lambda \bar{x}_t \Delta t + \sigma_\eta \sqrt{\Delta t} \varepsilon_{t+1}^\eta, \\ \varepsilon_{t+1}^\eta &\sim \mathcal{N}(0, 1).\end{aligned}$$

A.5 Price-Augmented Filtering (Robustness Variant)

Because prices are public and informative under (8), a fully consistent informational equilibrium would incorporate p into the observation set and solve a joint filtering/fixed-point problem. As

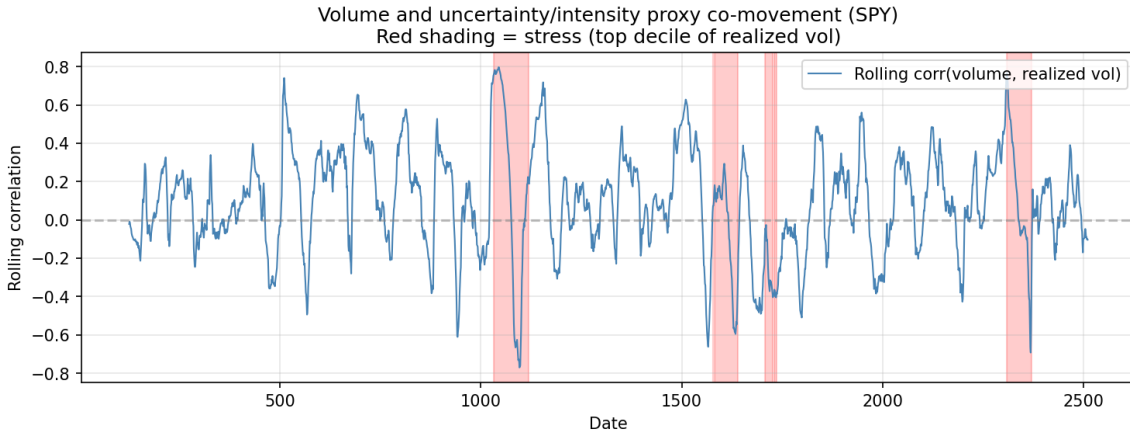


Figure 12: Rolling correlation of volume and realized volatility (SPY). Red shading = stress (top decile of realized vol).

Sample	Correlation	SE	<i>t</i> -stat
Full	0.296	0.019	15.826
Stress (top decile vol)	0.388	0.055	7.005
Non-stress	0.223	0.021	10.856

Table 18: Volume–volatility correlation: full sample, stress, and non-stress (Newey–West *t*-stats).

a robustness check aligned with the implemented Euler update above, we construct an *implicit* noisy observation of v_t from the realized price increment:

$$\tilde{v}_t^{(p)} := p_t + \frac{(p_{t+1} - p_t) - \lambda \bar{x}_t \Delta t}{\kappa \Delta t} = v_t + \frac{\sigma_\eta}{\kappa \sqrt{\Delta t}} \varepsilon_{t+1}^\eta.$$

Conditional on \mathcal{F}_t , this yields a Gaussian observation of v_t with measurement variance $R_p = \sigma_\eta^2 / (\kappa^2 \Delta t)$ (scaled by a factor $\sigma_{p,\text{obs}}^2$ in the code to probe robustness). We then apply an additional Kalman update using $\tilde{v}_t^{(p)}$ as a measurement (after processing the private signal), holding the state prediction fixed. Table 6 summarizes the impact of this price-consistent augmentation on the reported k -effects.

References

- Brad M. Barber and Terrance Odean. Boys will be boys: Gender, overconfidence, and common stock investment. *The Quarterly Journal of Economics*, 116(1):261–292, 2001. doi: 10.1162/003355301556400.
- Pierre Cardaliaguet and Charles-Albert Lehalle. Mean field game of controls and an application to trade crowding. *Mathematics and Financial Economics*, 12(3):335–363, 2018. doi: 10.1007/s11579-018-0206-7.
- René Carmona and François Delarue. *Probabilistic Theory of Mean Field Games with Applications I: Mean Field FBSDEs, Control, and Games*, volume 83 of *Probability Theory and Stochastic Modelling*. Springer, Cham, 2018a. doi: 10.1007/978-3-319-58920-6.

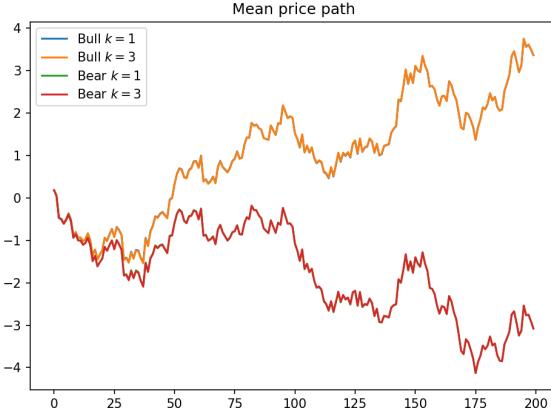


Figure 13: Mean price path across baseline scenarios (bull/bear regimes; $k \in \{1, 3\}$).

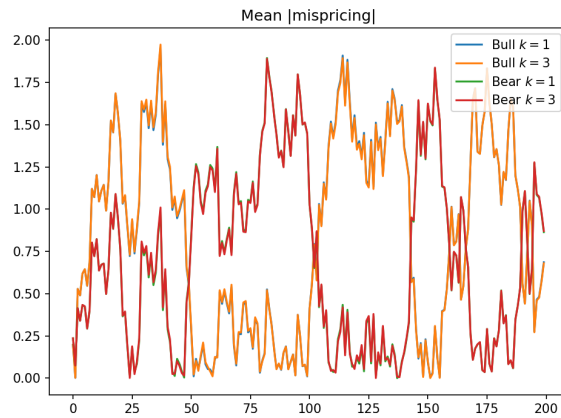


Figure 14: Mean absolute mispricing $\mathbb{E}[|p_t - v_t|]$ across baseline scenarios.

René Carmona and François Delarue. *Probabilistic Theory of Mean Field Games with Applications II: Mean Field Games with Common Noise and Master Equations*, volume 84 of *Probability Theory and Stochastic Modelling*. Springer, Cham, 2018b. doi: 10.1007/978-3-319-58973-1.

Rene Carmona, Jean-Pierre Fouque, and Li-Hsien Sun. Mean field games and systemic risk. *Communications in Mathematical Sciences*, 13(4):911–933, 2015. doi: 10.4310/CMS.2015.v13.n4.a4.

Kent Daniel, David Hirshleifer, and Avanidhar Subrahmanyam. Investor psychology and security market under- and overreactions. *The Journal of Finance*, 53(6):1839–1885, 1998. doi: 10.1111/0022-1082.00077.

J. Bradford De Long, Andrei Shleifer, Lawrence H. Summers, and Robert J. Waldmann. Noise trader risk in financial markets. *Journal of Political Economy*, 98(4):703–738, 1990.

Nicolas Fournier and Arnaud Guillin. On the rate of convergence in Wasserstein distance of the empirical measure. *Probability Theory and Related Fields*, 162(3):707–738, 2015. doi: 10.1007/s00440-014-0583-8.

Simon Gervais and Terrance Odean. Learning to be overconfident. *The Review of Financial Studies*, 14(1):1–27, 2001. doi: 10.1093/rfs/14.1.1.



Figure 15: Rolling volatility proxy (standard deviation of returns) across baseline scenarios.

Olivier Guéant, Jean-Michel Lasry, and Pierre-Louis Lions. Mean field games and applications. In *Paris-Princeton Lectures on Mathematical Finance 2010*, volume 2003 of *Lecture Notes in Mathematics*, pages 205–266. Springer, 2010. doi: 10.1007/978-3-642-14660-2_3.

Harrison Hong and Jeremy C. Stein. A unified theory of underreaction, momentum trading, and overreaction in asset markets. *Journal of Finance*, 54(6):2143–2184, 1999. doi: 10.1111/0022-1082.00184.

Minyi Huang, Roland P. Malhamé, and Peter E. Caines. Large population stochastic dynamic games: closed-loop McKean-Vlasov systems and the Nash certainty equivalence principle. *IEEE Transactions on Automatic Control*, 51(11):1730–1755, 2006. doi: 10.1109/TAC.2006.884922.

Aimé Lachapelle, Jean-Michel Lasry, Charles-Albert Lehalle, and Pierre-Louis Lions. Efficiency of the price formation process in presence of high frequency participants: a mean field game analysis. *Mathematics and Financial Economics*, 10(3):223–262, 2016. doi: 10.1007/s11579-016-0161-0.

Daniel Lacker. A general characterization of the mean field limit for stochastic differential games. *Probability Theory and Related Fields*, 165(3–4):581–648, 2016. doi: 10.1007/s00440-015-0641-9.

Daniel Lacker. On the convergence of closed-loop Nash equilibria for the infinite horizon mean-field LQG game. *ESAIM: Control, Optimisation and Calculus of Variations*, 24(2):437–469, 2018. doi: 10.1051/cocv/2017011.

Terrance Odean. Volume, volatility, price, and profit when all traders are above average. *The Journal of Finance*, 53(6):1887–1934, 1998. doi: 10.1111/0022-1082.00078.